VAPOUR-LIQUID EQUILIBRIA FOR ARGON-METHANE SYSTEM

by

KALYAN KUMAR MAITRA

A thesis submitted in partial fulfillment of the requirement for the degree of Master of Science in the Department of Chemical Engineering University of Ottawa 1966

Thesis Author

Research Director

ABSTRACT

An apparatus for the determination of vapour-liquid equilibrium data at low temperatures was built and employed.

The vapour-liquid equilibrium data for the argon-methane system were obtained at three isothermal conditions, namely, at 122.66, 132.52 and 143.16°K.

The experimental equilibrium data were correlated with two constant Redlich-Kister equations.

The liquid phase fugacity coefficients for pure methane were calculated from the experimental data.

An attempt was made using the theory of interaction and cavitation to predict the Henry's law constants.

ACKNOWLEDGEMENT

The author is very much indebted to Dr. B. C.-Y. Lu for directing the research work, for invaluable advice, especially on various problems during the experimental work as well as the theoretical study.

Mr. S.-D. Chang, a graduate student in the department, helped in setting up the apparatus.

The author is very grateful to Messrs. F. Ciacobbi and G. Gasperetti for their technical assistance in constructing the apparatus.

Mr. M. P. Pleet of the Division of Fuels and Mining Practice, High Pressure Chemistry, Mines and Technical Department, Government of Canada, assisted with patience in the calibration of the pressure gauges. Also acknowledged is the Mines Department for the facilities available for calibration of the gauges.

TABLE OF CONTENTS

LIST OF FIGURES

LIST OF TABLES

NOMENCLATURE

A	=	constant
a	=	hard sphere diameter of a molecule
a_{12}	=	distance of closest approach of solvent and solute molecules or the radius of the sphere around solute molecule which excludes centers of solvent molecules
B_{ii}	=	second virial coefficient
B, C, D	=	constants of Redlich-Kister equation
E_i	=	molal interaction energy
f	=	fugacity
$g(r)$	=	radial distribution function
G	=	molal Gibbs free energy
$\bar{G}_i$	=	partial molal Gibbs free energy of interaction
$\bar{G}_c$	=	partial molal Gibbs free energy of cavitation
$\bar{g}_i$	=	partial molecular Gibbs free energy of interaction
$\bar{g}_c$	=	partial molecular Gibbs free energy of cavitation
K_H	=	Henry's Law constant
k	=	Boltzmann's constant
K	=	equilibrium ratio
N_i	=	number of molecules of i th component
$\tilde{N}$	=	Avogadro's number
P	=	total pressure
P_c	=	critical pressure
P_R	=	reduced pressure
R	=	Gas Law constant = $k \times \tilde{N}$
S_i	=	molal entropy of interaction
T	=	temperature
T_c	=	critical temperature

T_R	=	reduced temperature
V	=	volume
v	=	molal volume
x	=	mole fraction in the liquid phase
y	=	mole fraction in the vapour phase
γ	=	activity coefficients at the solution temperature and pressure $\gamma_i \to 1$ as $x_i \to 1$
ϕ	=	fugacity coefficient, f_i/P, for mixtures $(\bar{f}_i/y_i P)$ or $(\bar{f}_i/x_i P)$
ϕ^o	=	fugacity coefficient in the liquid phase at the system conditions for the pure components
ρ	=	number density, molecules/cc
δ_{ij}	=	second virial cross coefficient for i and j components in the binary mixture
ω	=	acentric factor
σ_{12}	=	distance of the closest approach for the solute and solvent molecules in L.-J. potential equivalent to a_{12}
ϵ_i	=	energy of interaction per molecule
μ	=	chemical potential
$\wedge$		indicates molal property in the mixture
—		indicates the partial molal quantity
Subscript 1		Argon
2		Methane
Superscript o		indicates saturation conditions
*		indicates $P \to o$, ideal state
L		property of the liquid
V		property of the vapour

INTRODUCTION

The vapour-liquid equilibrium data are useful for the separation of gases from gaseous mixtures. The data may be obtained experimentally or by prediction.

The prediction methods have been developed in classical thermodynamics by evaluating the fugacity coefficients with the help of a suitable equation of state. However, a suitable equation of state is not available for both vapour and liquid phases, for a wide range of temperature and pressure.

A new approach may be visualised for studies of the behaviour of molecules in mixtures. It is based on energy of interaction between molecules and energy required to create a cavity for the solute molecule in the solvent. It seems that the data on simple non-polar mixtures would be most suitable for this kind of studies. By means of statistical thermodynamic analysis, equations have been developed to obtain the chemical potential of the components in the vapour and liquid mixtures. In engineering calculations the advantage of such equations may be taken. The Henry's law constant at infinite dilution may be calculated, then using the integrated Gibbs-Duhem equation the activity coefficient for the complete concentration range may be calculated.

Even in the early stage, this approach

encounters difficulties in calculating the radial distribution function, and in turn the interaction energy. It seems that further work in this field should be promising.

Object of the Work:

The first phase of this work was concerned with building a suitable apparatus for low temperature measurements.

The isothermal data were considered more valuable than isobaric measurements (31). For studying the effect of temperature at least three isotherms were needed. It was planned to obtain data for three isotherms around 120 to 140° K for the argon-methane system. Argon and methane are considered simple molecules due to their molecular structure (or shape).

The liquid phase fugacity coefficients for pure methane were not available for a wide range of temperature and pressure in the literature. It was decided to calculate the fugacity coefficients from the experimental data.

It was also intended to predict the results using the molecular theory.

LITERATURE SURVEY

The low temperature vapour-liquid equilibrium studies have been well discussed in the literature (2, 38, 39).

In this work a brief review is made regarding the experimental procedure, the calculation methods for correlation of data and prediction.

Experimental methods:

Various experimental methods are proposed for measuring vapour-liquid equilibrium data at low temperatures.

The dew point and bubble point determination method is employed by Sage and Lacey (34, 35) for determining the vapour-liquid equilibria, by Bloomer and Parent (1) at low temperatures. In this method the gases of known composition are fed into the equilibrium apparatus. The vapour and liquid samples need not be analyzed. The disadvantage is that it may involve much personal error in determining the temperature and pressure at which the first dew or bubble formed.

The static method is utilised by Fedoritenko and Ruhemann (12) at low temperatures. Cheung and Wang (4) have also used a static equipment at low temperatures. In this method a mixture of gases is placed in the equilibrium cell and maintained at constant temperature

for a long time. Then the samples are taken and analysed. This method requires an exceptionally long time and may encounter error during sampling, as the pressure may change from the equilibrium pressure.

The flow method is utilised by Sutaman and Brown (41) for multicomponent gas mixtures. A gas mixture is passed through an equilibrium cell maintained at constant temperature and is partially liquefied. The samples are withdrawn and analysed continuously. The disadvantage lies in the maintenance of constant pressure and temperature during rapid condensation.

The forced circulation method is developed by Inglis (16), modified and used by Dodge and Dunbar (18). Davis, Rodewald and Kurata (7) modified the equipment further. This method is widely used at present. In this the vapour is recirculated back into the liquid using a pump. Thus the equilibrium is reached very quickly. The vapour and liquid samples can be withdrawn almost without disturbing the equilibrium. This method is utilised in the present investigation and discussed in detail later.

Calculation methods, correlation and prediction of data:

The experimental vapour liquid compositions at equilibrium may be directly represented by a plot of equilibrium ratios. For the purpose of correlation the fugacity coefficient may be calculated for the components in the mixture from an equation of state. The activity coefficients may be calculated from the experimental composition values and represented by suitable equations. An infinite dilution model with the aid of molecular theory may be used for calculation of limiting values of the activity coefficient and in turn for the whole range of composition.

These methods are discussed in brief in this section. The molecular theory is discussed in Appendix VI.

The equilibrium ratio:

The equilibrium ratio is defined as,

$$K_i = y_i/x_i \qquad (1)$$

The plots of logarithmic values of equilibrium ratio, as functions of the logarithmic values of the total pressure, are frequently used as means of representation.

For gaseous mixtures, which follow Raoult's Law,

$$y_i P = x_i P^\circ \qquad (2)$$

or

$$K_i = \frac{y_i}{x_i} = \frac{P^\circ}{P} \qquad (3)$$

In this case, if the logarithmic values of K_i are plotted against logarithmic values of total pressure at constant temperature, it should have a slope of minus one. Deviation would occur for non-ideal cases.

Fugacity coefficients of the components:

The fugacity of the i th component in the mixture at constant temperature is defined as,

$$d\mu_i = RT\, d\ln \bar{f}_i, \quad \mu_i = \mu_i^\circ + RT \ln \bar{f}_i \tag{4}$$

So that,

$$\text{as } P \longrightarrow 0 \quad \frac{\bar{f}_i}{x_i P} \longrightarrow \frac{\bar{f}_i^*}{x_i P^*} \longrightarrow 1$$

At equilibrium:

$$d\mu_i^V = d\mu_i^L \tag{5}$$

So, $$\bar{f}_i^V = \bar{f}_i^L \tag{6}$$

Now, $$\bar{f}_i^V = \hat{\phi}_i^V y_i P \tag{7}$$

$$\bar{f}_i^L = \hat{\phi}_i^L x_i P \tag{8}$$

Therefore, from (7) and (8)

$$\frac{y_i}{x_i} = \frac{\hat{\phi}_i^L}{\hat{\phi}_i^V} \tag{9}$$

The fugacity of the i th component in the vapour mixture can be calculated from the Redlich-Kwong (27) equation of state or virial coefficients. But the calculation of the fugacity coefficient in the liquid mixture is not possible at the present stage due to the lack of a suitable equation of state. So this method is not employed in this investigation.

The evaluation of activity coefficients and correlation:

Various direct and indirect methods are available for the prediction of activity coefficients.

The activity coefficient of the i th component in the solution is

$$\gamma_i = \frac{\bar{f}_i}{x_i f_i} \tag{10}$$

as $$x_i \longrightarrow 1 \quad \bar{f}_i \longrightarrow f_i \tag{11}$$

and so $$\gamma_i \longrightarrow 1 \tag{12}$$

where the pure component at the solution temperature, pressure and the same physical condition is the standard state.

At equilibrium,

$$\bar{f}_i^V = \hat{\phi}_i^V y_i P \tag{13}$$

$$= \bar{f}_i^L$$

$$= \gamma_i^L x_i f_i^L \tag{14}$$

Equating (13) and (14)

$$\gamma_i^L = \frac{y_i}{x_i} \frac{\hat{\phi}_i^V P}{f_i^L} \tag{15}$$

Again,

$$f_i^L = P \nu_{oi} \tag{16}$$

where, ν_{oi} = pure component liquid phase fugacity coefficient at the solution temperature and pressure.

Substituting (16) in (15)

$$\gamma_i^L = \frac{y_i}{x_i} \frac{\hat{\phi}_i^V}{\nu_{oi}} \tag{17}$$

Several methods (14, 36a, 43, 45) are available for calculation of liquid phase activity coefficients.

Hildebrand and Scatchard (14) proposed

$$RT \ln \gamma_i = V_i \phi_2^2 (\delta_1 - \delta_2)^2 \tag{18}$$

where V_1 is the molar volume of component one in the liquid, ϕ_2 is the volume fraction of the component two, and δ_1 and δ_2 are the solubility parameters of the two components.

The solubility parameters may be evaluated from the energy of vapourisation, in turn from $\Delta H^V - RT$, where ΔH^V is the heat of vapourisation.

$$\delta \cong \left(\frac{\Delta H^V - RT}{V}\right)^{1/2} \tag{19}$$

Other methods are given in the literature (14) to evaluate the solubility parameter. In this method a very simplified model of "regular solution" is assumed and in many cases far from the actual mixing process.

At low pressures the fugacity coefficients of the vapour phase may be determined from the second virial coefficient. Hence the activity coefficient (43) may be evaluated as,

$$\ln \gamma_i^L = \ln \frac{y_i P}{x_i P_i^*} + \frac{(B_{ii} - V_i^L)(P - P_i^*)}{RT} + \frac{P \delta_{ij} y_j^2}{RT} \tag{20}$$

The calculation based on Equation 17 is possible if some reliable values are obtained for the gas phase fugacity and the liquid phase fugacity.

$$\gamma_i^L = \frac{y_i}{x_i} \frac{\hat{\phi}_i^V}{\phi_{oi}} \qquad (17)$$

y_i and x_i are obtained from experimental values. The vapour phase fugacity coefficient of the i th component in the binary mixture can be calculated by the Redlich-Kwong equation of state (27). The Redlich-Kwong equation of state is modified further (28, 29) based on the acentric factor for different molecules. The acentric factor is defined by Pitzer (21), as:

$$\omega = - \log P_r - 1.000 \qquad (21)$$

P_r is the reduced vapour pressure at reduced temperature equal to 0.7.

The acentric factor for argon and methane as reported by Pitzer (22) are -0.002 and 0.013. respectively.

From the values of accentric factor of argon and methane it follows that argon and methane can be assumed simple fluids without much error (23, 24) and the values of vapour phase fugacity coefficients for both the gases in the mixture can be calculated from the Redlich-Kwong equation of state.

The problem lied mainly in obtaining the values of ϕ_o, i.e., the liquid phase fugacity coefficient for the pure components at the system conditions. Many authors (3, 46) have published values of ϕ_o at acentric factor equal to zero.

At constant temperature,

$$\ln \varphi_2 - \ln \varphi_2^{\circ} = \frac{1}{RT} \int_{P^{\circ}}^{P} (v^L - \frac{RT}{P})\, dP \qquad (22)$$

The molar volume of the liquid can be considered constant for a low pressure change. Integrating Equation 22

$$\ln \frac{\varphi_2}{\varphi_2^{\circ} P^{\circ}} = \frac{1}{RT} v^L (P - P') \qquad (23)$$

Then φ_2 at the desired pressure,

$$\varphi_2 = \frac{f^L}{P} e^{\frac{v^L (P - P')}{RT}} \qquad (24)$$

Using the above equation and obtaining values of f^L at saturation pressure from Pitzer's data (22., 46) the values of φ_2 are calculated and plotted in Figure 1. A comparison of the values of liquid phase fugacity coefficients calculated using different methods are shown in Figure 2. The curve four is based on the extrapolated values of Chao-Seader (3).

In the present work Equation 17 is used to calculate the activity coefficients of argon utilising the calculated values of φ_2 based on Pitzer's (46) data at saturation.

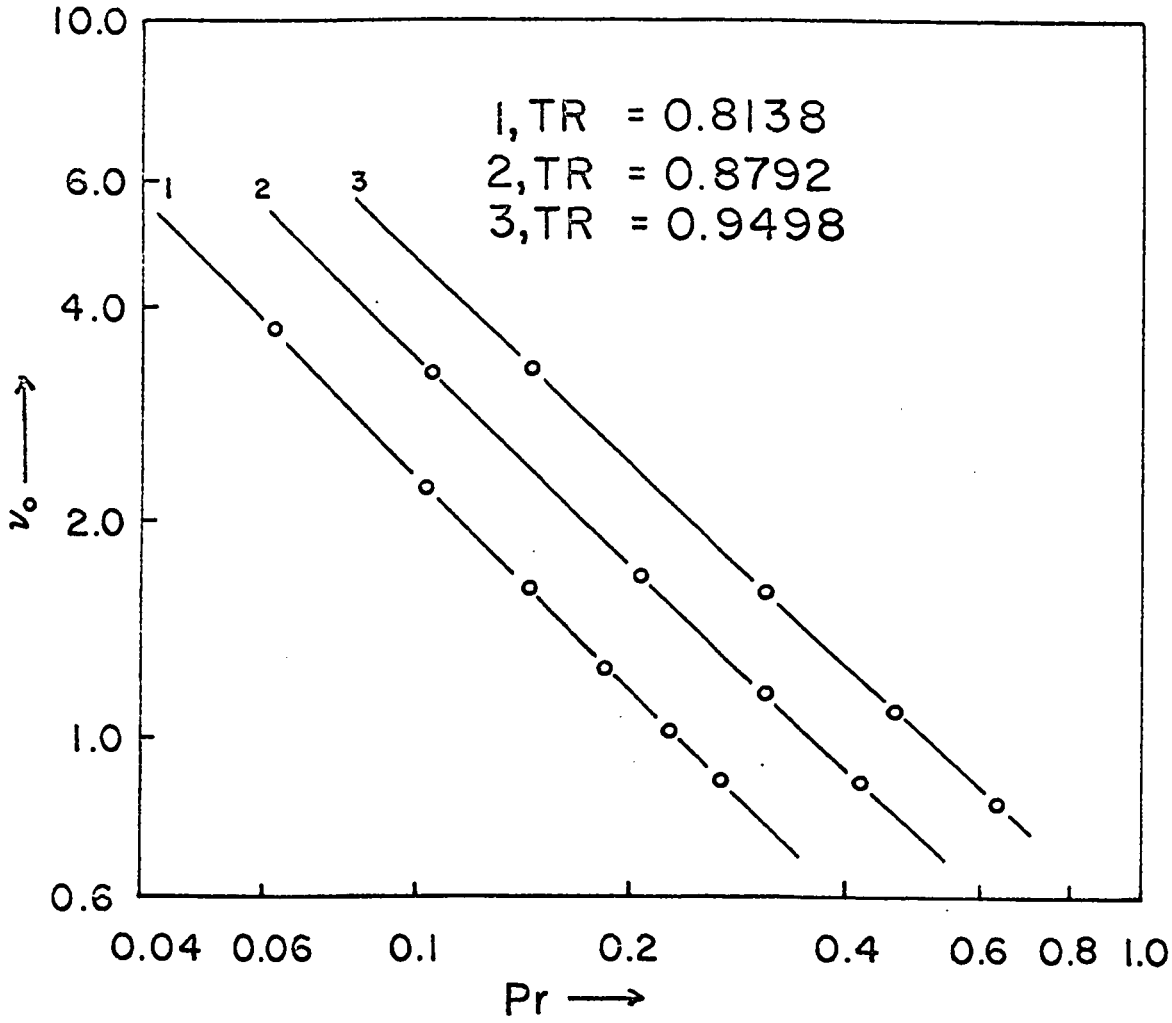

Fugacity coefficient of pure argon in the liquid phase

Fig. 1

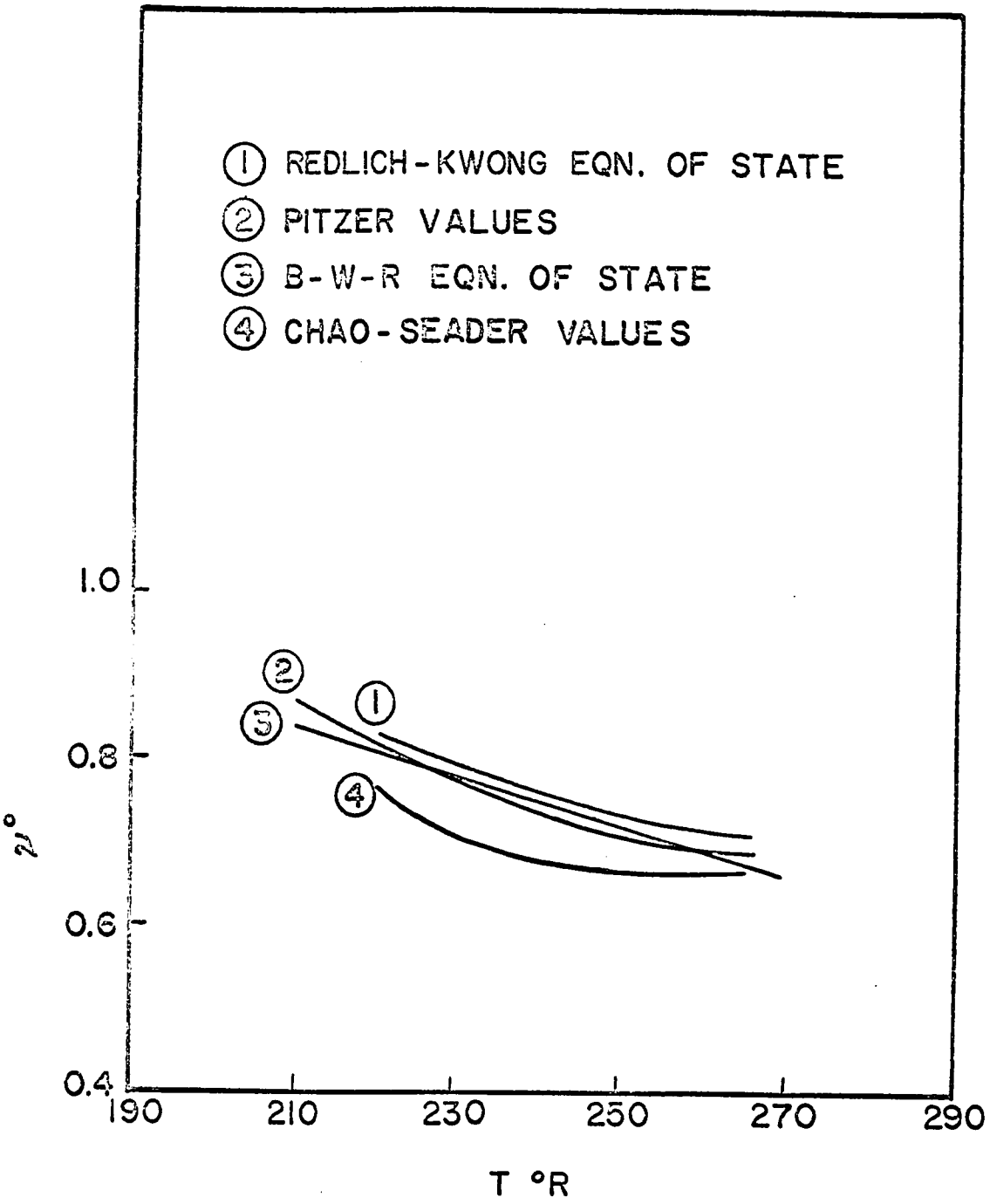
① REDLICH-KWONG EQN. OF STATE
② PITZER VALUES
③ B-W-R EQN. OF STATE
④ CHAO-SEADER VALUES
1.0
0.8
0.6
0.4
2°
190
210
230
250
270
290
T °R

Fig. 2

Representation of activity coefficient:

Different empirical forms for representing the liquid phase activity coefficients are proposed (26, 30, 36, 43, 45). It is found that the activity coefficients are conveniently represented by a power series (30) such as:

$$\ln \gamma_1 = x_2^2 \left[B - C(4x_2 - 3) + D(2x_2 - 1)(6x_2 - 5) + \text{-----} \right] \quad (30)$$

$$\ln \gamma_2 = x_1^2 \left[B + C(4x_1 - 3) + D(2x_1 - 1)(6x_2 - 5) + \text{-----} \right] \quad (31)$$

EXPERIMENTAL DETAILS

The experiments were performed using 99.996% pure Argon and 99.9% pure Methane. Detailed analyses of the gases are shown in Appendix II.

The apparatus was designed to operate from room temperature to -160°C and up to 1200 psig pressure with isopentane as the bath liquid.

The apparatus shown in the schematic diagram (Fig. 3) comprised of the following sections: the equilibrium cell, the feeding and evacuation device, the low temperature bath, the electromagnetic pump, the temperature control and measuring system, the sampling device for the vapour and liquid and the sample analysing arrangement.

The equilibrium cell:

The equilibrium cell was made of 306 stainless steel. The inside diameter was 3/8 inch and the length was 6 inches. The thermocouple well, the vapour line and the liquid sampling tube were welded to the cover plate. The cover plate was screwed on the main body of the cell with 1/8 inch teflon packing placed between them.

The thermocouple well was sealed at the top using a Swagelok connection. The vapour inlet line was coiled and welded through an

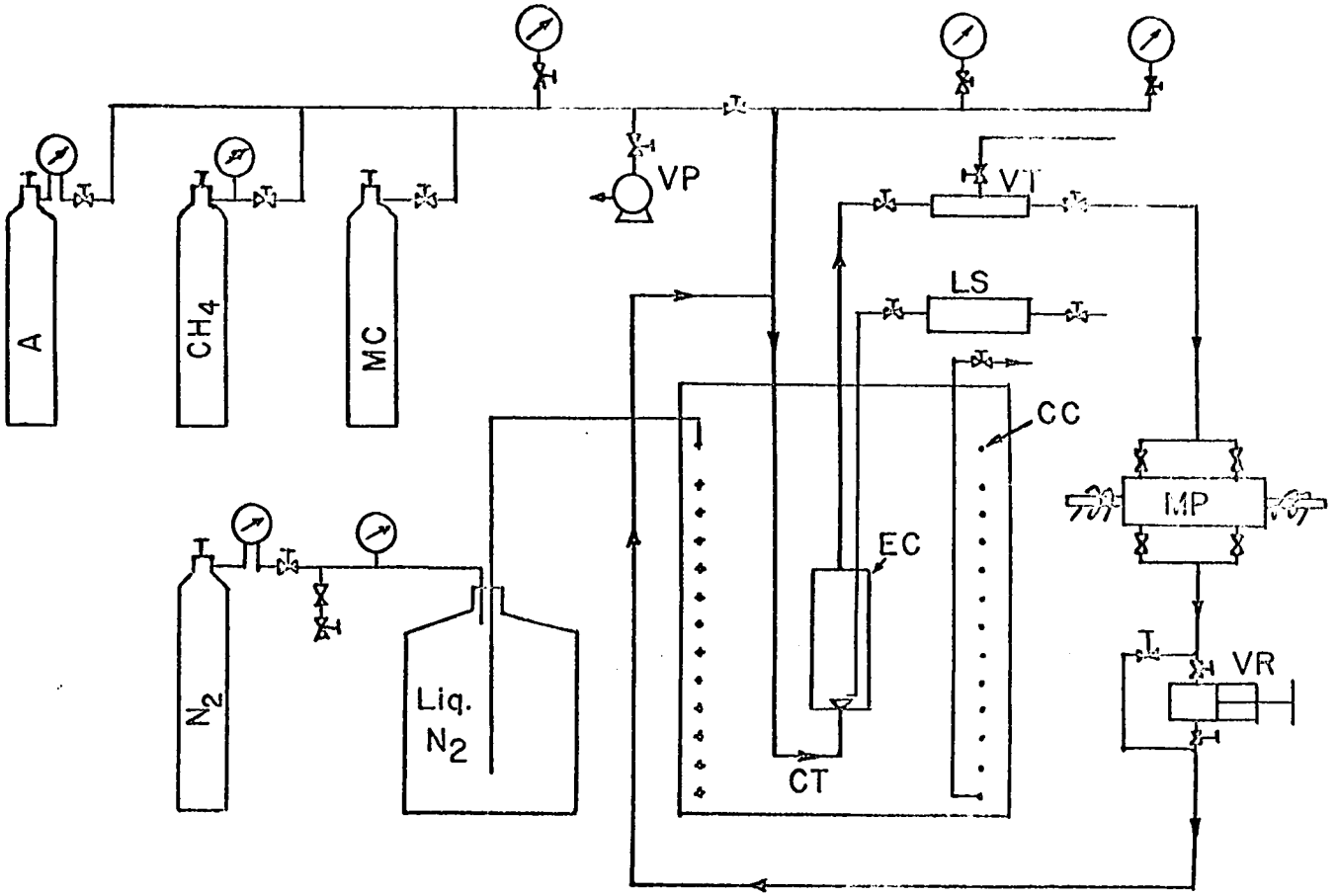

VT Vapour sampling tube
CT Cryostat
EC Equilibrium cell
LS Liquid sampling bulb
CC Bath cooling coils
MP Magnetic pump
VR Volume regulator
VP Vacuum pump
MC Mixing chamber

The schematic diagram of the forced-recirculation apparatus

Fig. 3

Autoclave joint to the bottom of the cell. A sprayer with twenty tiny holes sprayed the vapour inside the equilibrium cell. Two screens, one near the top and the other near the bottom, were used to reduce entrainment and to distribute the vapour.

The feeding and evacuation devices:

The equilibrium cell, the recirculation loop and the sampling tubes were evacuated to one-hundredth of a millimeter mercury before each run using a vacuum pump.

The gases were charged in two different processes. Either the gases were premixed and then fed into the system or charged one after the other. Argon was withdrawn from the cylinder through a pressure regulator. A needle valve and a gauge were connected with the methane cylinder. A small empty cylinder with a pressure gauge was mounted in series and was used as a premixing chamber.

The low temperature bath:

The low temperature bath is shown in more detail in Figure 4. An enameled Dewar flask was placed inside an aluminum vessel leaving one inch air gap all around the flask. The aluminum vessel was insulated with two-inch thick fiber glass all around.

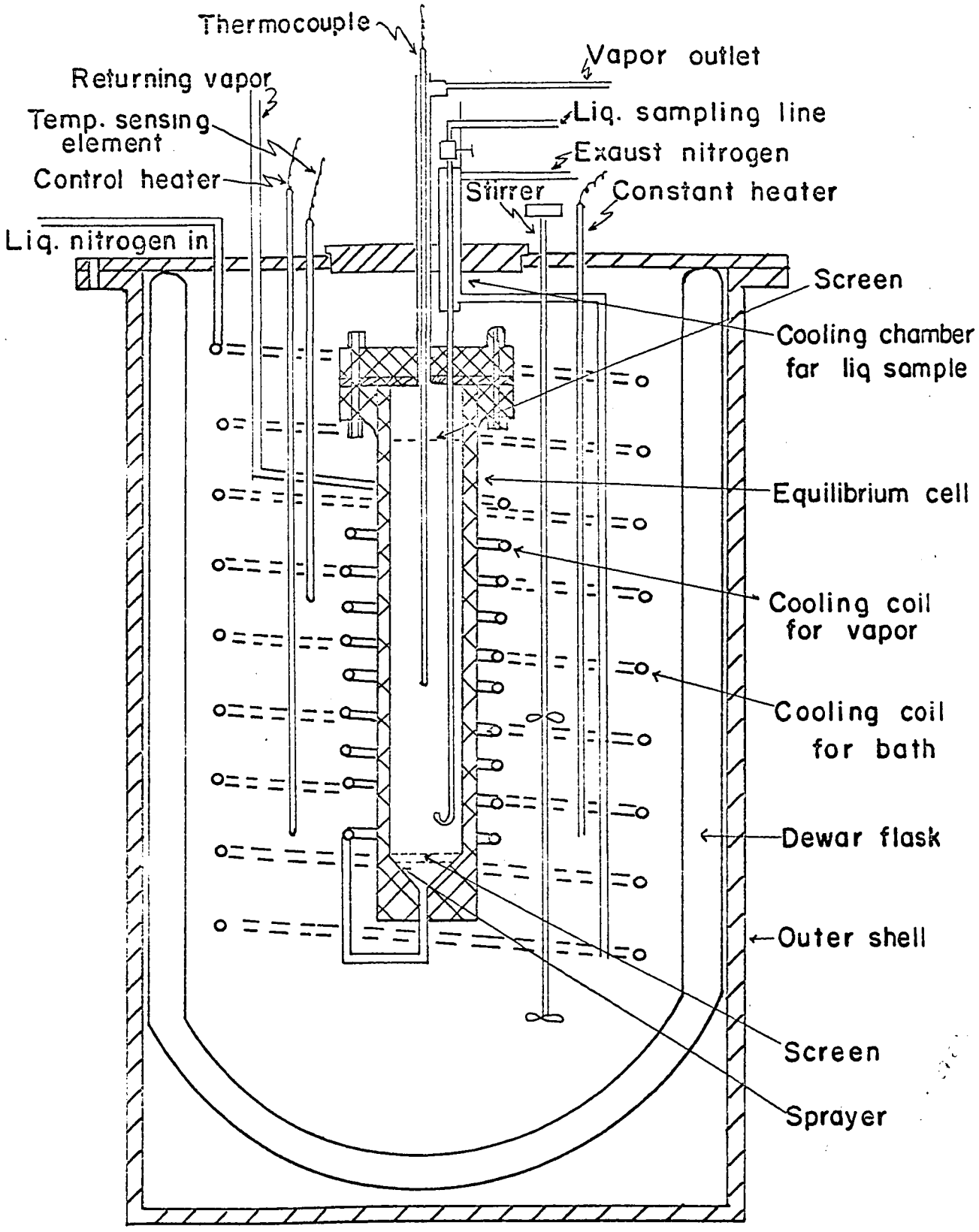

The schematic diagram of the equilibrium cell and the cryostat

Fig. 4

Isopentane (freezing point -160° C) used as the bath liquid, was placed in the flask and was cooled by evaporating liquid nitrogen in copper coils. Liquid nitrogen was withdrawn from a tank under nitrogen gas pressure through a foam insulated quarter-inch copper tube. The cooling coils were fitted to the lid of the bath.

The bath was heated using an immersion heater (resistance 20 ohms) connected to the power source through a powerstat. Another one used as a controlling heater was connected through the temperature controller. A speed adjustable stirrer was used to stir the bath liquid.

All the connections were made through the top cover of the bath. The top cover was insulated by glass fiber and foam insulator.

The electromagnetic pump:

For the recirculation of the vapour an electromagnetic pump was used. The pump was built in the laboratory. It was the same as that used by Chang (5) with slight modification. A condenser and a high resistance were connected across the D.C. output to reduce the electrical pressure on the relays.

The pump was a double acting piston type. The piston (made of Alnico-5 magnet) moved to and fro, due to the induced magnetic field.

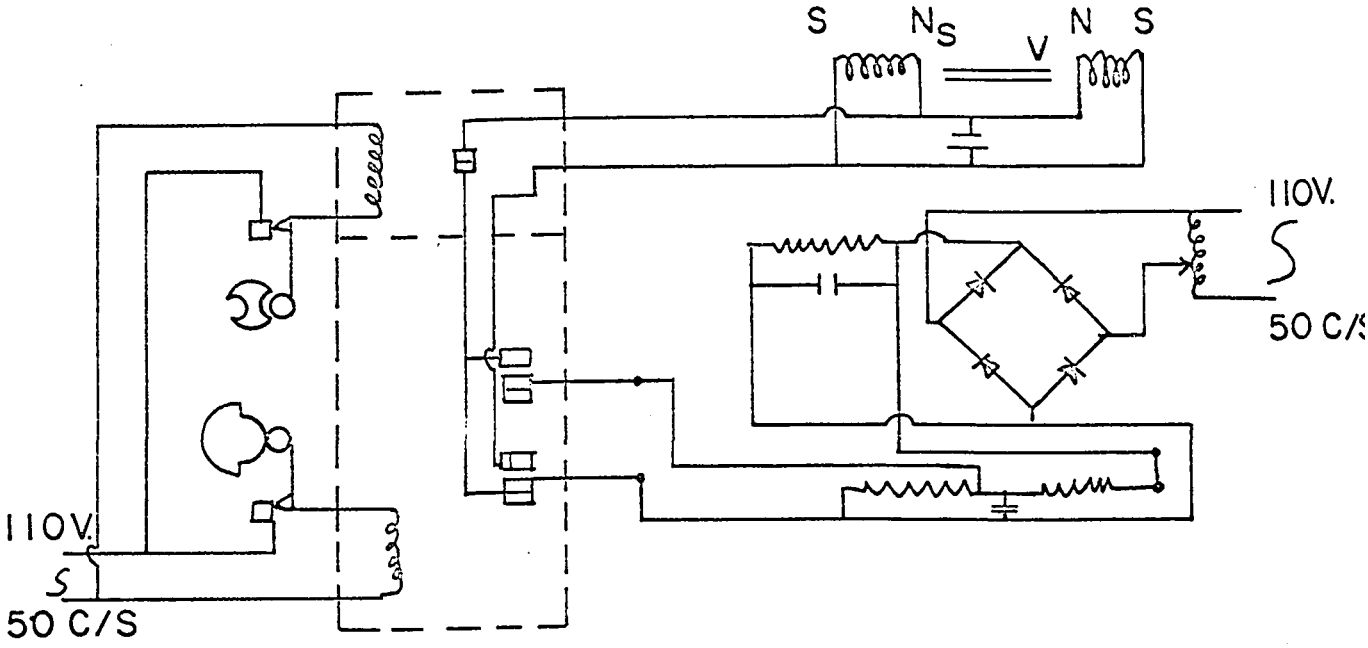

The electrical circuit of the electromagnetic pump

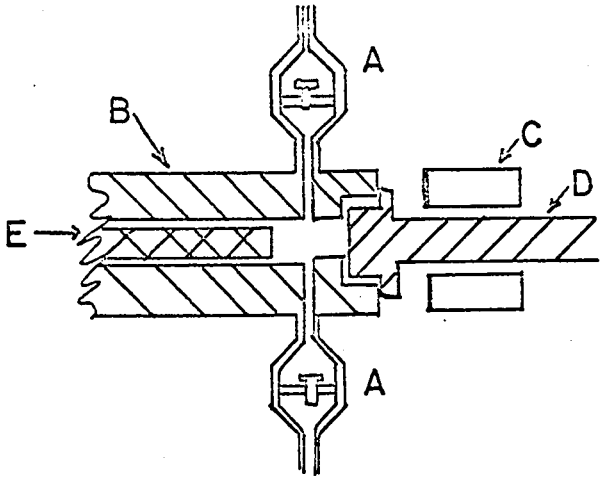

A = Check valve
B = Pump body
C = Coils
D = Soft iron core
E = Magnet

Pump cross section

Fig. 5

The magnetic field was created by current passing through the coils having soft iron core. The pump capacity was 0 to 50 cc. per min. The pressure drop across the pump was 1 to 6 psi.

The circuit diagram and the pump cross-section are shown in Figure 5.

The temperature control and measurement:

The bath was cooled to a slightly lower temperature than desired by regulating the flow of the liquid nitrogen and adjusting the voltage of one immersion heater. The controlling heater connected through a Bayley temperature controller model 250 with resistance sensing element maintained the required temperature. The temperature controller had a guaranteed accuracy up to $\pm$ 0.001° C. The temperature was measured by copper-constantan thermocouple placed inside the equilibrium cell. The reference junction was place inside an ice bath. The millivoltage was measured with a Tinsley Potentiometer which read up to 0.0001 mV.

The bath temperature was maintained almost steady and fluctuated only $\pm$ 0.02° C as registered by the thermocouple.

Calibration of the thermocouple is shown in Appendix III.

Measurement of pressure:

The pressure was measured using two test pressure gauges (Bourdon type), one of range 0 - 1500 psig with 5 psig divisions and the other of range 0 - 600 psig with 2 psig divisions.

The pressure gauges were calibrated using a dead weight tester. The calibration table for the 600 psig gauge is given in Appendix III.

Sampling of vapour and liquid:

The vapour samples were arrested in the vapour sampling tube by closing the valve at both ends of the tube. Difficulties were encountered with the liquid sampling procedure. No suitable description of the technique was available in the literature. In this work the following steps were developed. The capillary tube for liquid sampling was cooled with the evaporating nitrogen (which was almost at the bath temperature). The capillary tube was connected with a three-way valve. The first portion of the liquid was purged out. Then the sample was taken in the sampling tube and evaporated completely. The sampling tube was about 100 cc in capacity and was at room temperature. The flash vapourisation of the sample was avoided in this way.

Analysis of vapour and liquid:

The vapour and the liquid samples were analysed by a Perkin-Elmer Vapour Fractometer Model 154C along with a Speedomax potentiometric recorder. Two one-meter long columns, packed with silica gel (28 - 30 mesh) were used. Helium, the carrier gas, was flown at 7.5 psig pressure and at a rate of 41 cc per minute. The column temperature was 50°C. The chart speed of the recorder was one inch per minute. A typical analysis is shown in Figure 6. The argon and methane peak were quite apart.

The calibration of the gas chromatograph is shown in Appendix III.

Experimental procedure:

The equilibrium cell was evacuated to one-hundredth of a millimeter mercury. The bath was cooled to the required temperature. The gases were charged. The pump was switched on for circulation. The gases were circulated till the pressure and temperature were steady for an hour. The pump was stopped and after about fifteen minutes the vapour and liquid samples were collected. The samples were analysed with the calibrated chromatograph.

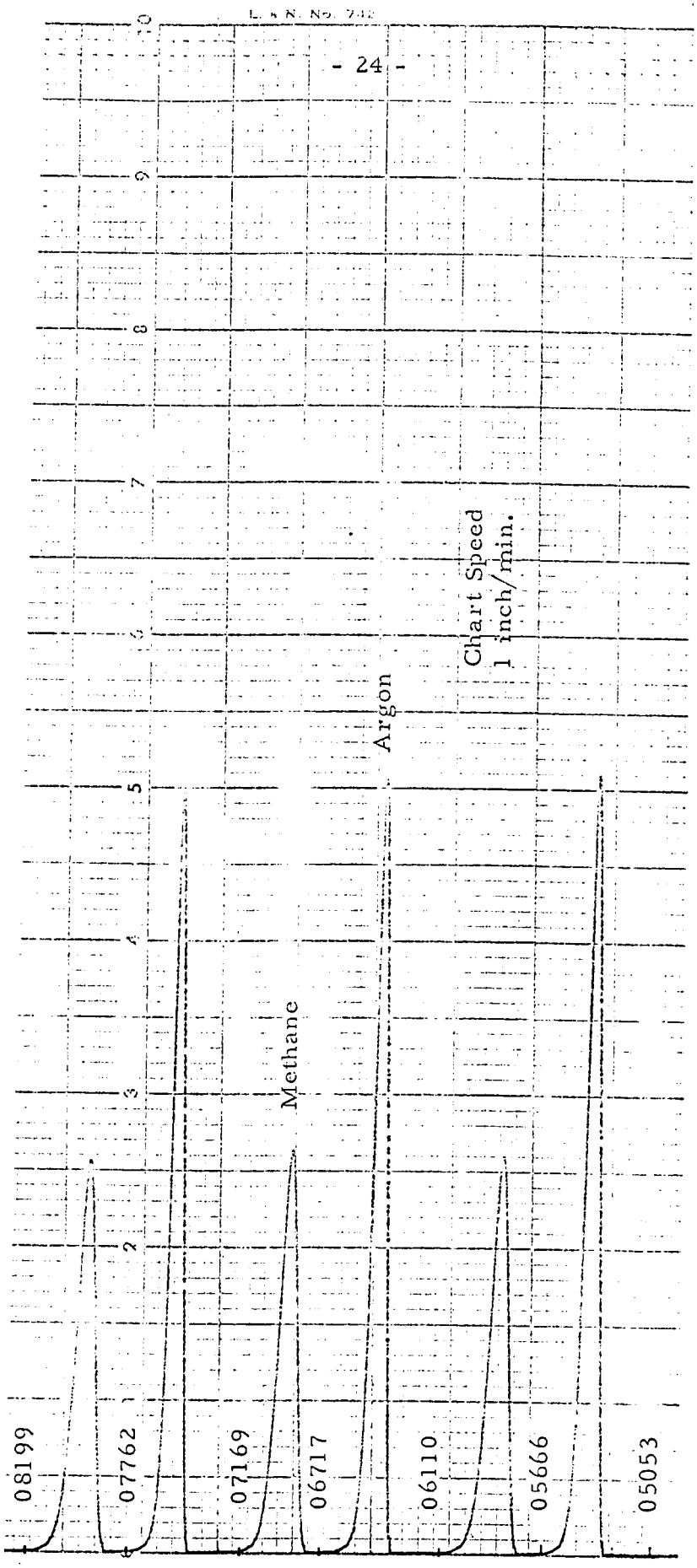

Fig. 6 Chromatogram

RESULTS

The experimental results are tabulated in Tables 1, 2 and 3, in Appendix I. The P - x - y and y - x diagrams are shown in Figures 7 to 13. The equilibrium ratios are plotted against pressure in a log-log scale in Figure 14.

The pressure was read up to $\pm$ 0.25 psi. The temperatures reported are accurate up to $\pm$ 0.02° C. The prepared mixture showed that the analytical procedure was capable of measuring up to $\pm$ 0.2 mole % in the composition range 20 to 80 mole %.

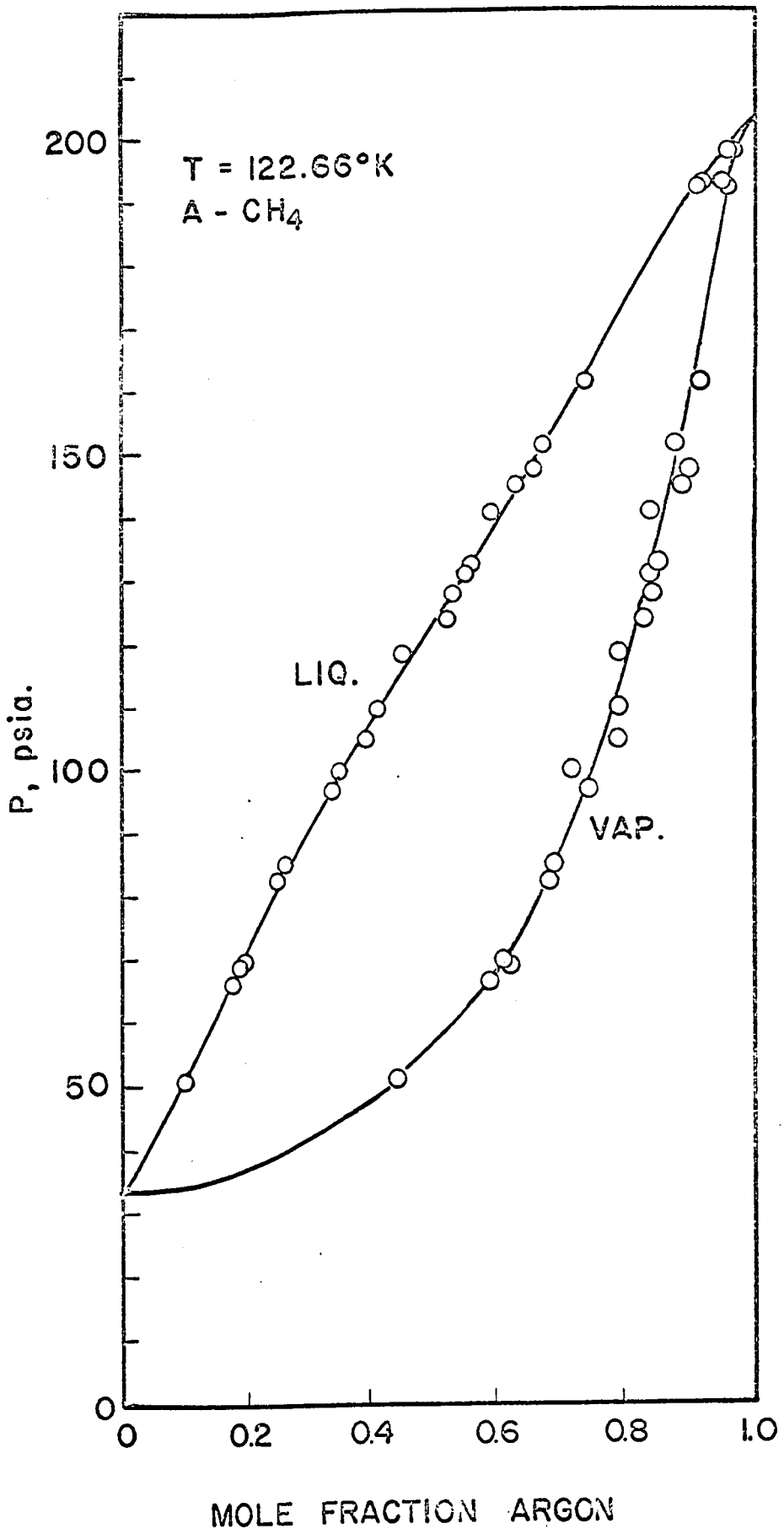
T = 122.66°K
A - CH4
LIQ.
VAP.
P, psia.
200
150
100
50
0
0
0.2
0.4
0.6
0.8
1.0
MOLE FRACTION ARGON

Fig. 7

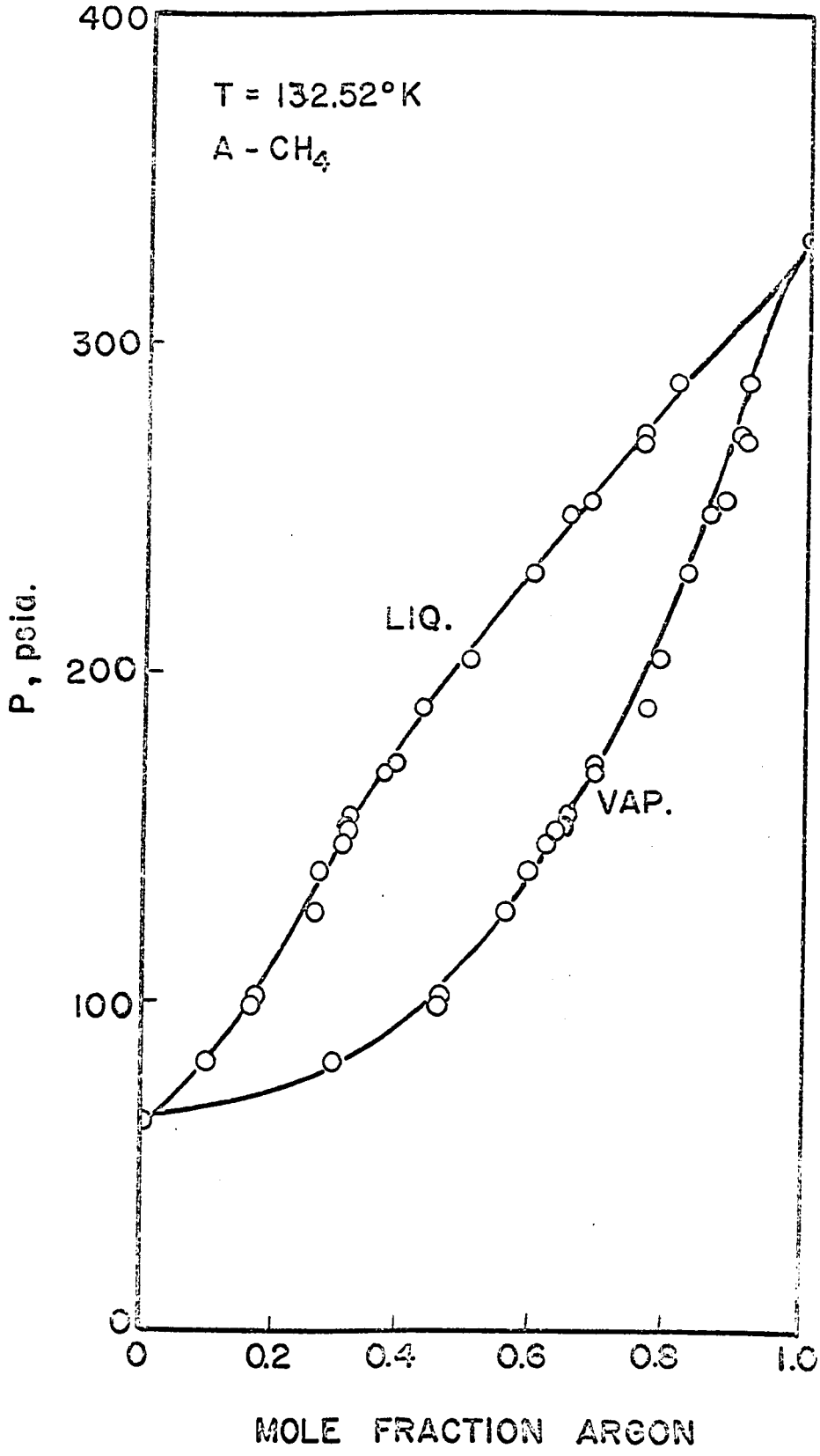
400
300
200
100
0
P, psia.
T = 132.52°K
A - CH_4
LIQ.
VAP.
0
0.2
0.4
0.6
0.8
1.0
MOLE FRACTION ARGON

Fig. 8

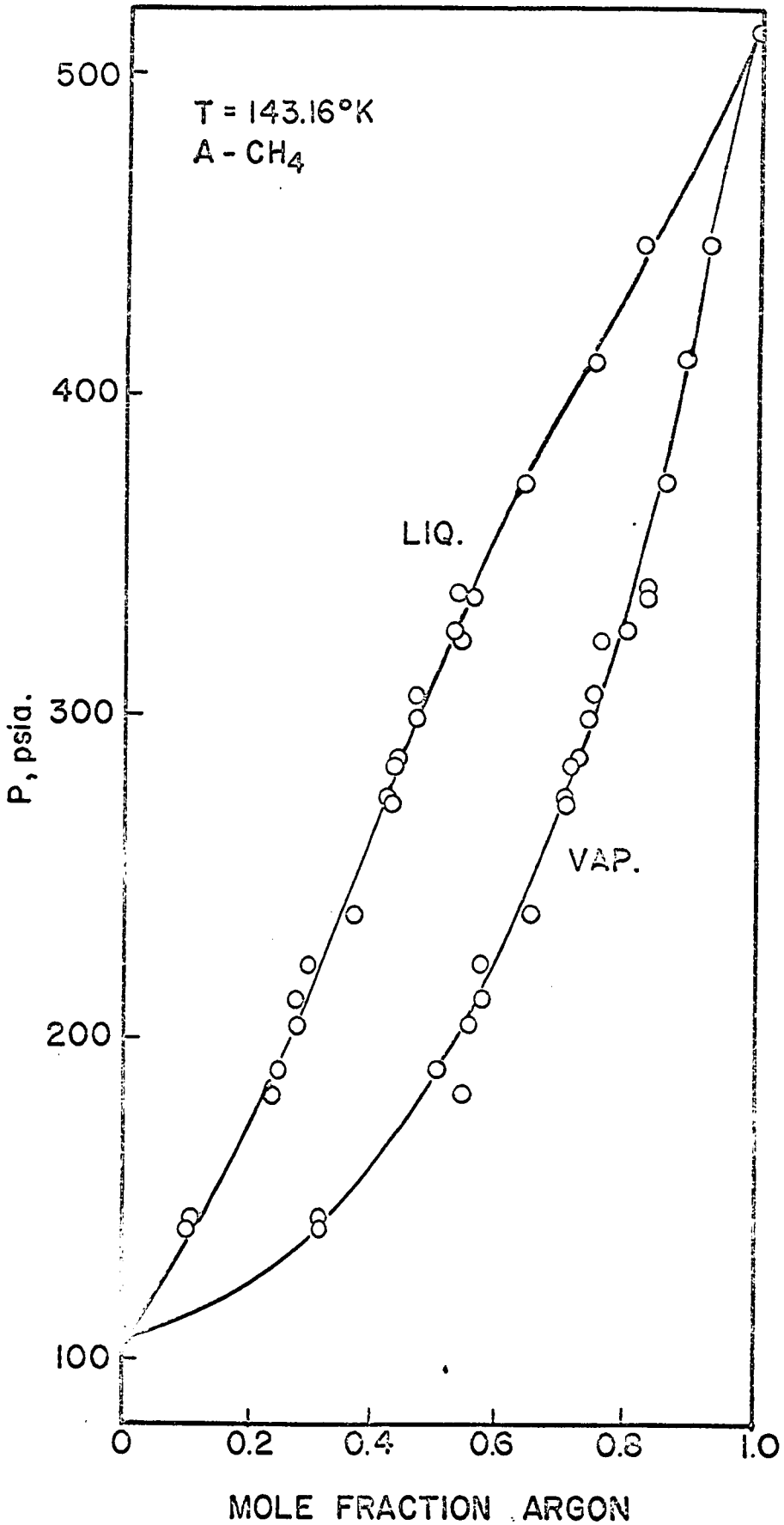
T = 143.16°K
A - CH4
LIQ.
VAP.
P, psia.
500
400
300
200
100
0
0.2
0.4
0.6
0.8
1.0
MOLE FRACTION ARGON

Fig. 9

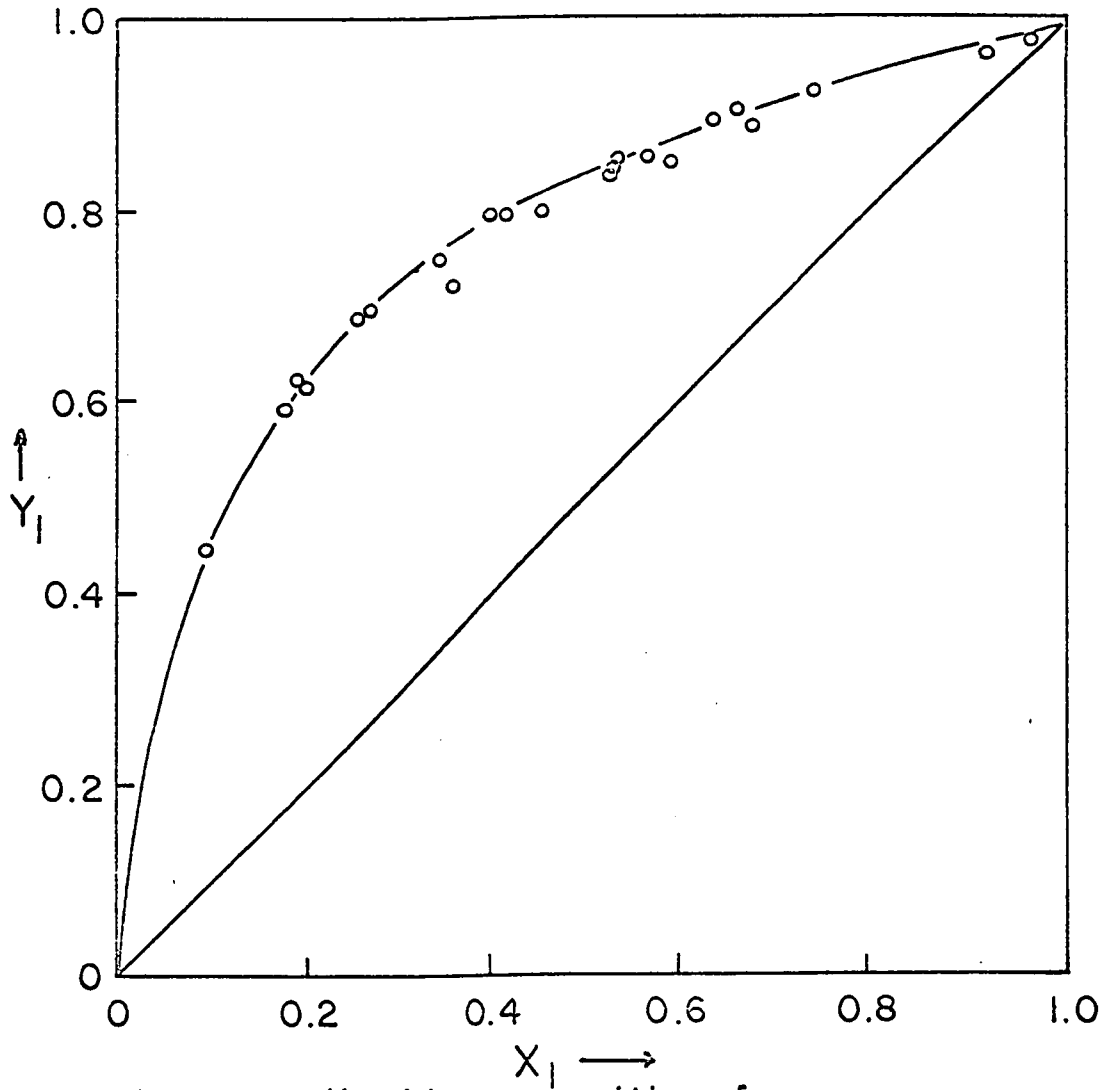

Vapour-liquid composition for argon at 122.66 °K

Fig. 10

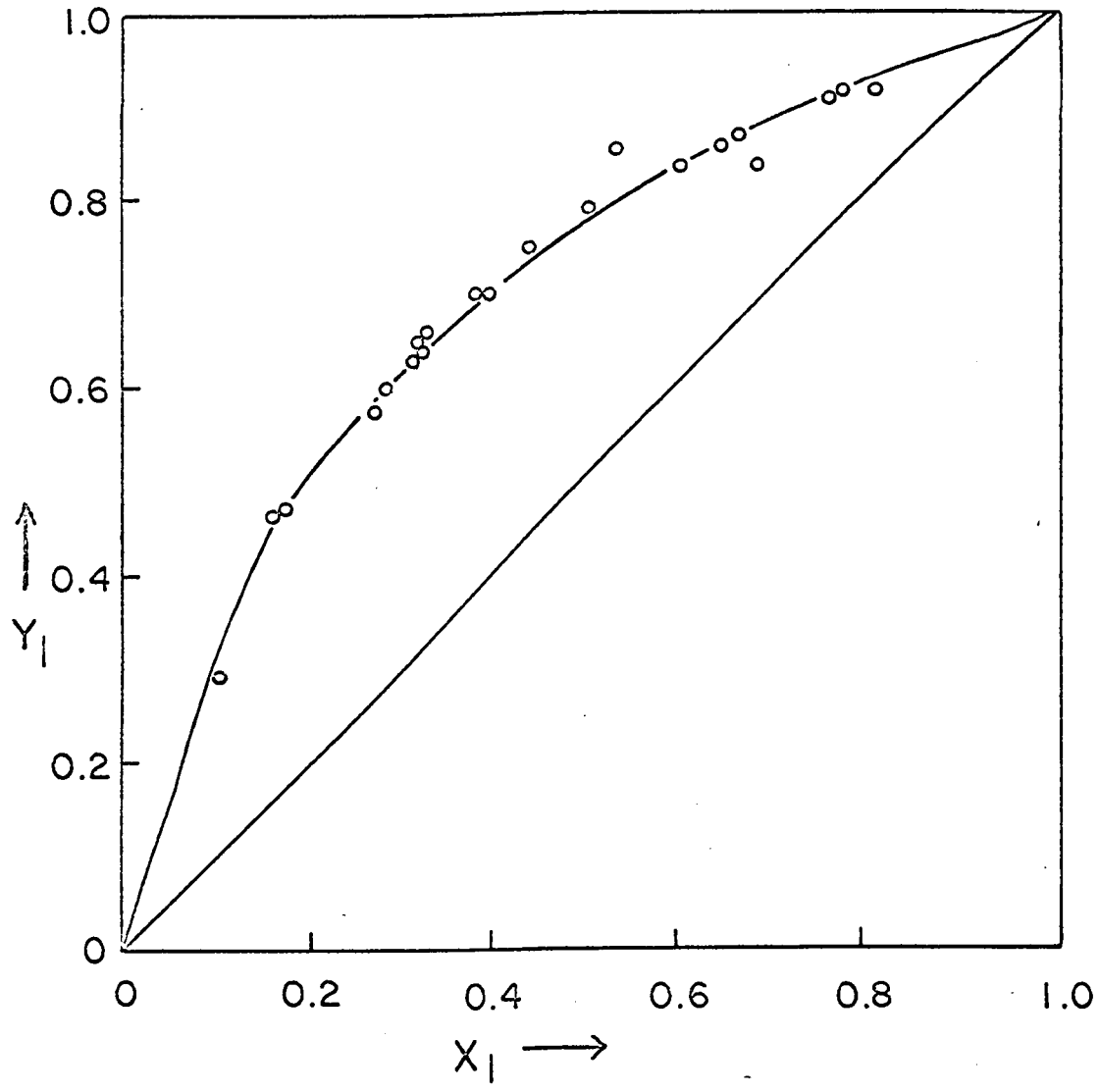

Vapour-liquid composition for argon at 132.52 °K

Fig. 11

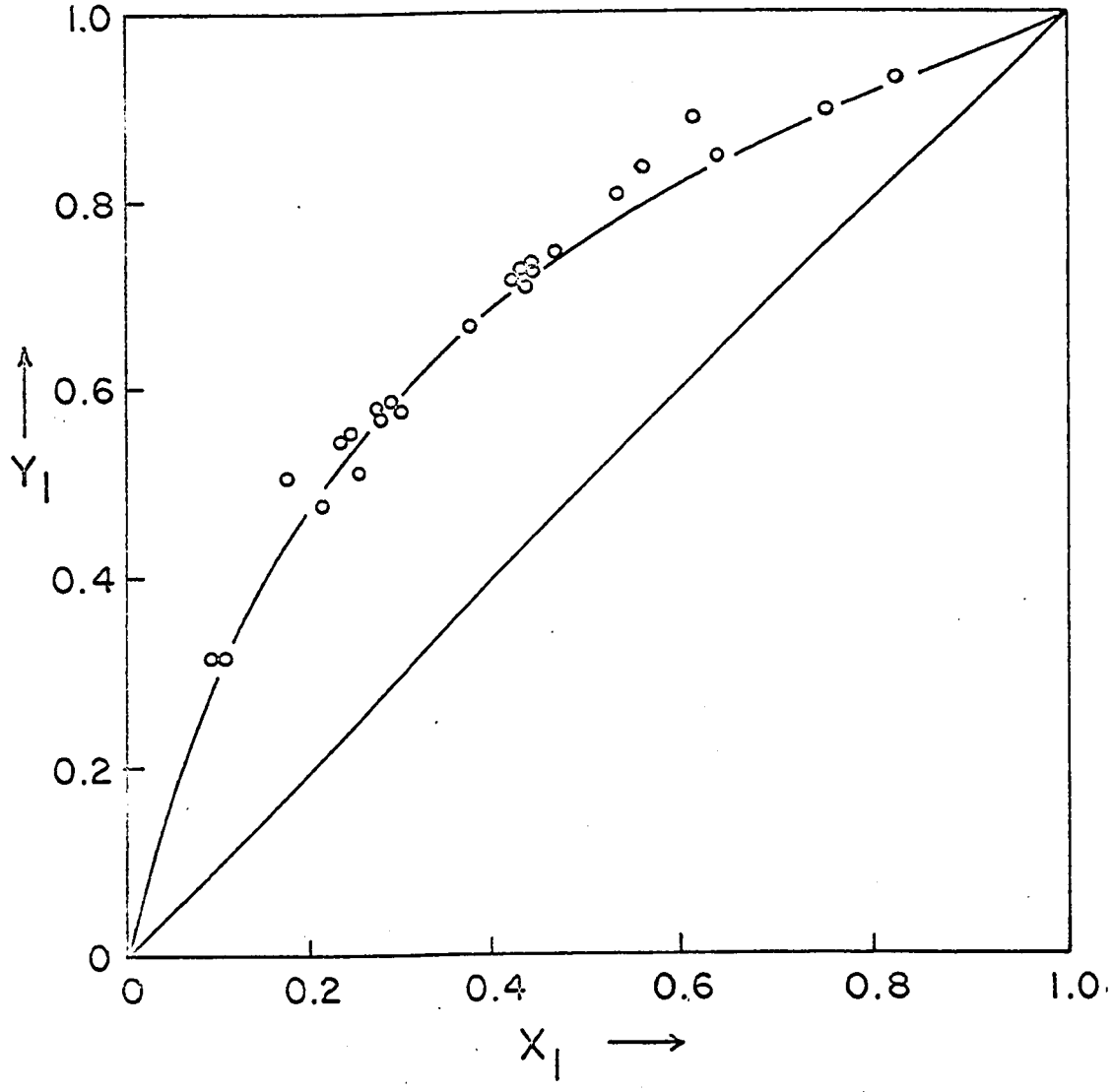

Vapour-liquid composition for argon at 143.16 °K

Fig. 12

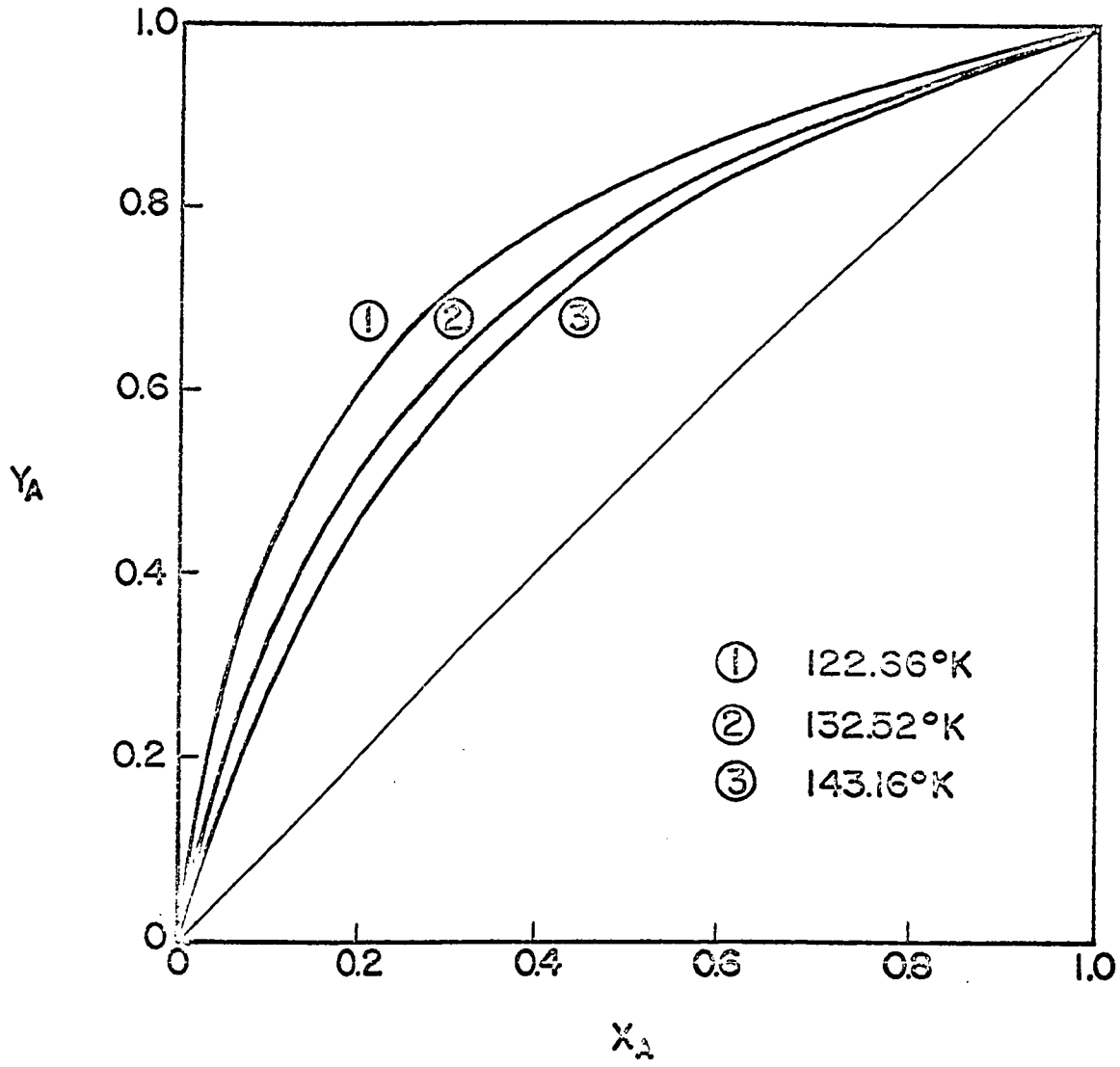

Fig. 13

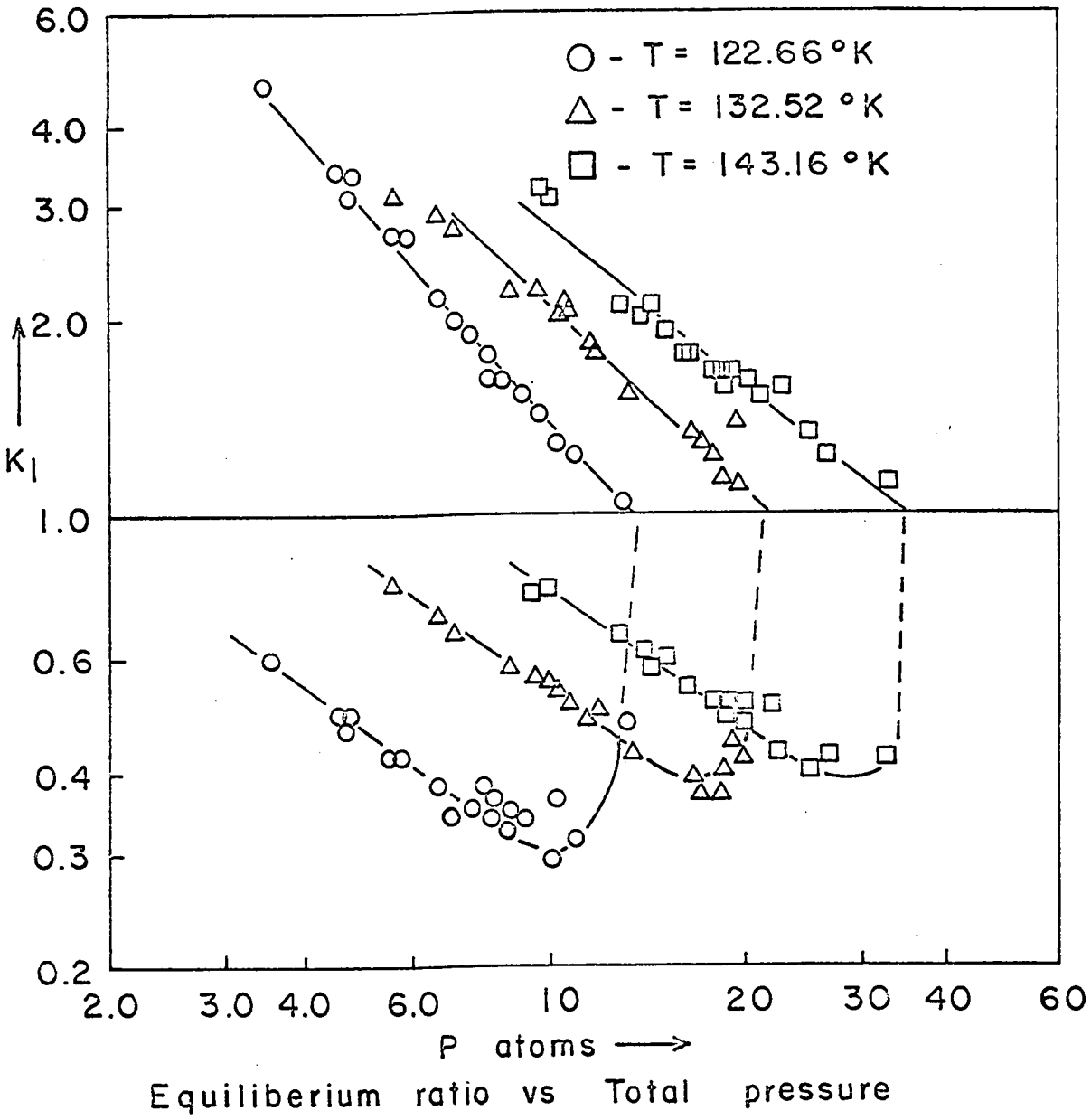
O - T = 122.66 °K
△ - T = 132.52 °K
□ - T = 143.16 °K
6.0
4.0
3.0
2.0
1.0
0.6
0.4
0.3
0.2
K1
2.0
3.0
4.0
6.0
10
20
30
40
60
P atoms ⟶
Equiliberium ratio vs Total pressure

Fig. 14

CORRELATION OF DATA

The activity coefficients for argon were calculated based on the equation:

$$\gamma_i = \frac{y_i}{x_i} \frac{\hat{\phi}_i^V}{\phi_i^o}$$

where y_i and x_i were obtained from experimental data. The fugacity coefficients in the liquid phase of pure argon were obtained from Figure 1. The fugacity coefficient for the vapour phase was calculated by the Redlich-Kwong equation of state (27). An available computer program was utilised in this calculation. The activity coefficients are tabulated in Tables 5, 6 and 7.

Recently Sprow and Prausnitz (37) published vapour liquid equilibrium data for the argon-methane system at 90.67° K. Their correlation indicated that the data might be well represented by a two-constant Redlich-Kister equation (30). In the present work, as the available data (19) for the liquid phase fugacity coefficient of pure methane were not dependable (6, 25), the correlations of the activity coefficient were made based on the activity coefficients of argon.

The two-constant Redlich-Kister equations (30) are given as follows:

$$\log \gamma_1 = x_2^2 \left[B + C (3x_1 - x_2) \right]$$

$$\log \gamma_2 = x_1^2 \left[B + C (x_1 - 3x_2) \right]$$

These expressions may be rearranged as:

$$\frac{\log \gamma_1}{x_2^2} = (B - C) + 4Cx_1$$

and

$$\frac{\log \gamma_2}{x_1^2} = (B + C) - 4Cx_2$$

The values of constants are obtained by using the least squares' method.

The values of the constants are obtained as follows:

Temperature	B	C
122.66° K	0.18434	0.01521
132.52° K	0.14597	0.01315
143.16° K	0.13652	0.01282

The values of $(\log \gamma_1)/x_2^2$ are plotted against x_1 in Figure 15. In the present calculations the values of $\log \gamma_1$ for argon are used to obtain the constants.

The activity coefficients for methane were then calculated based on the constants. The curves are shown in Figures 16 to 18.

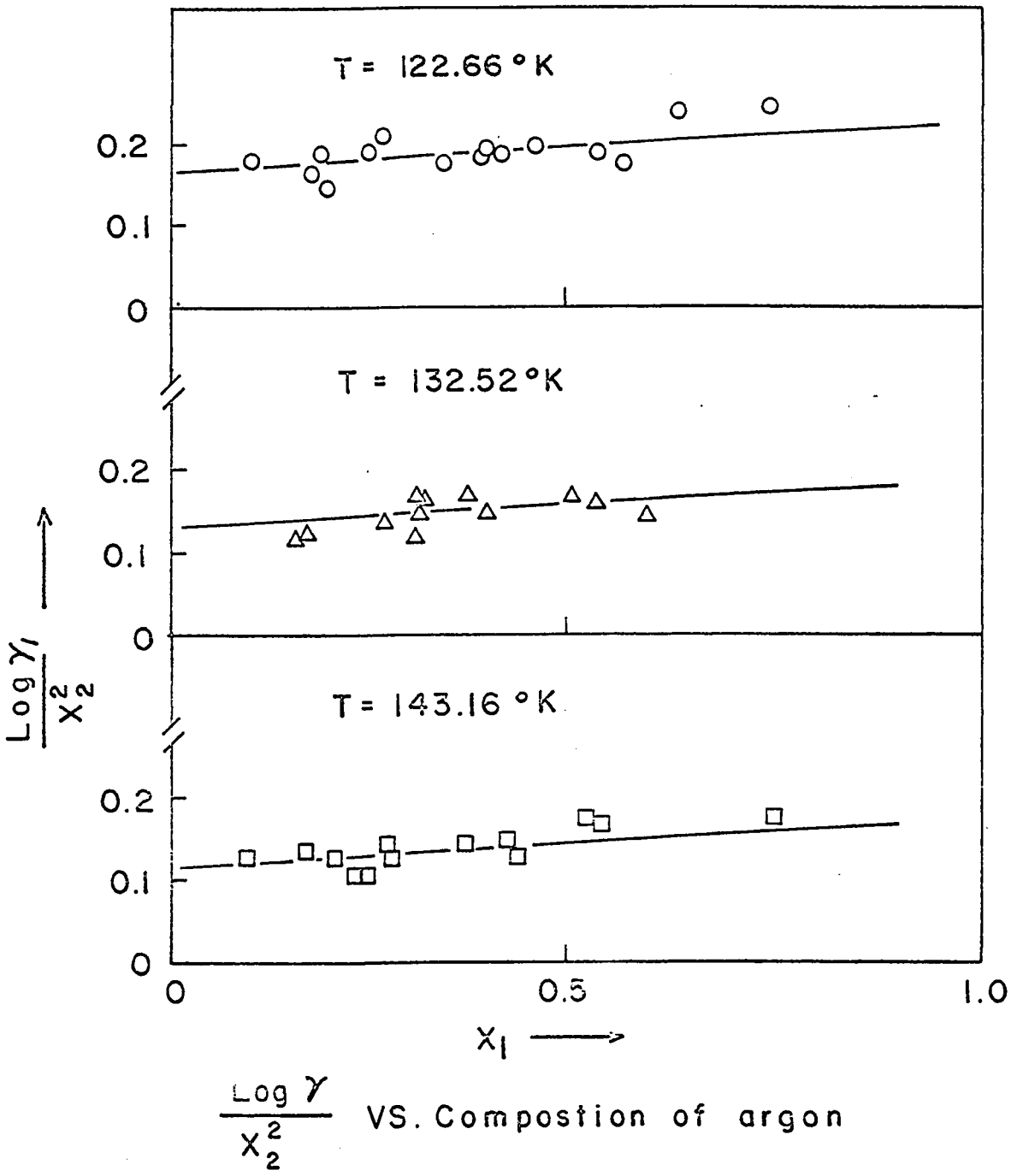

$\frac{\text{Log } \gamma}{X_2^2}$ VS. Compostion of argon

Fig. 15

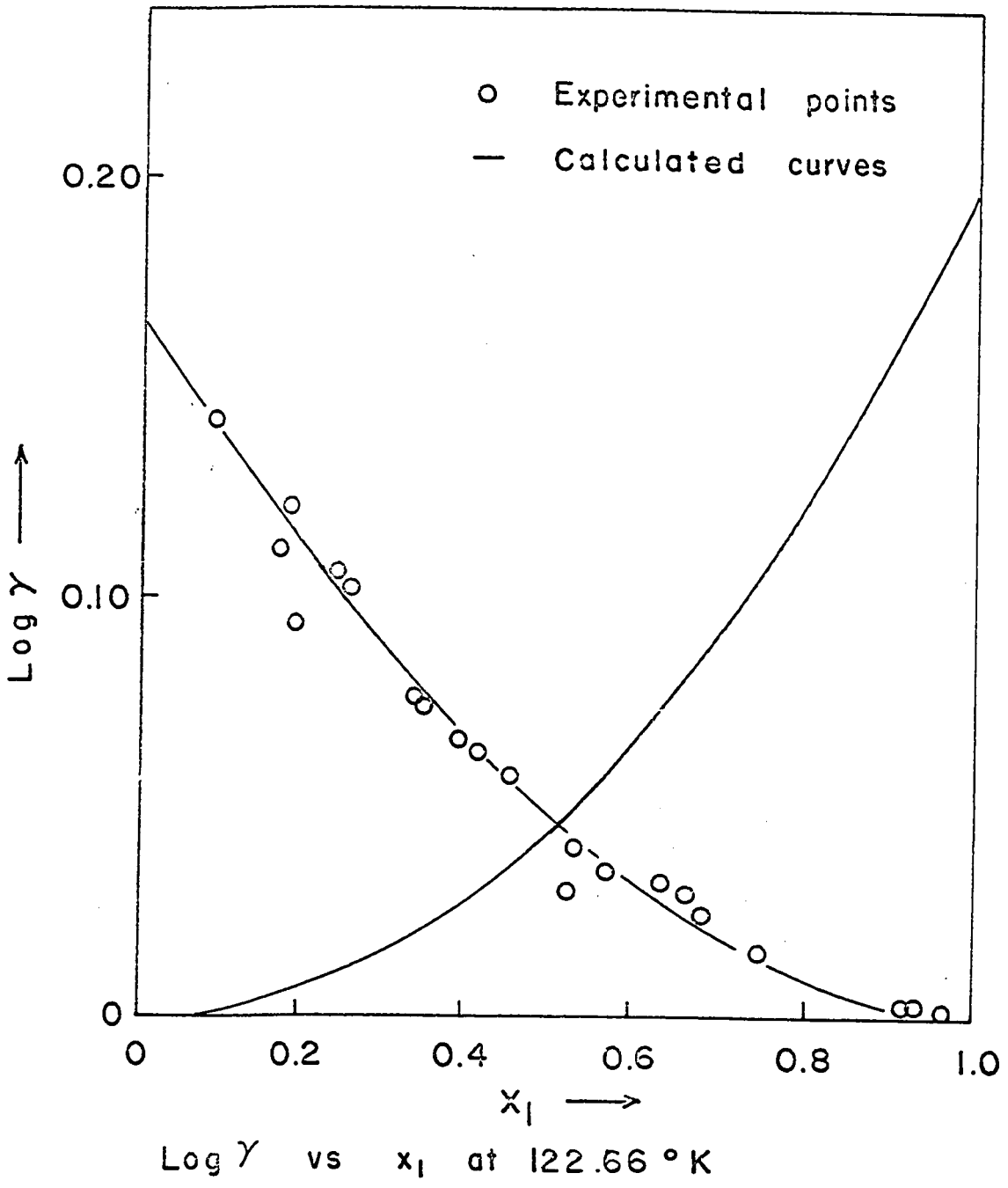
Experimental points
Calculated curves
0.20
0.10
0
Log γ
0
0.2
0.4
0.6
0.8
1.0
x1
Log γ vs x1 at 122.66 °K

Fig. 16

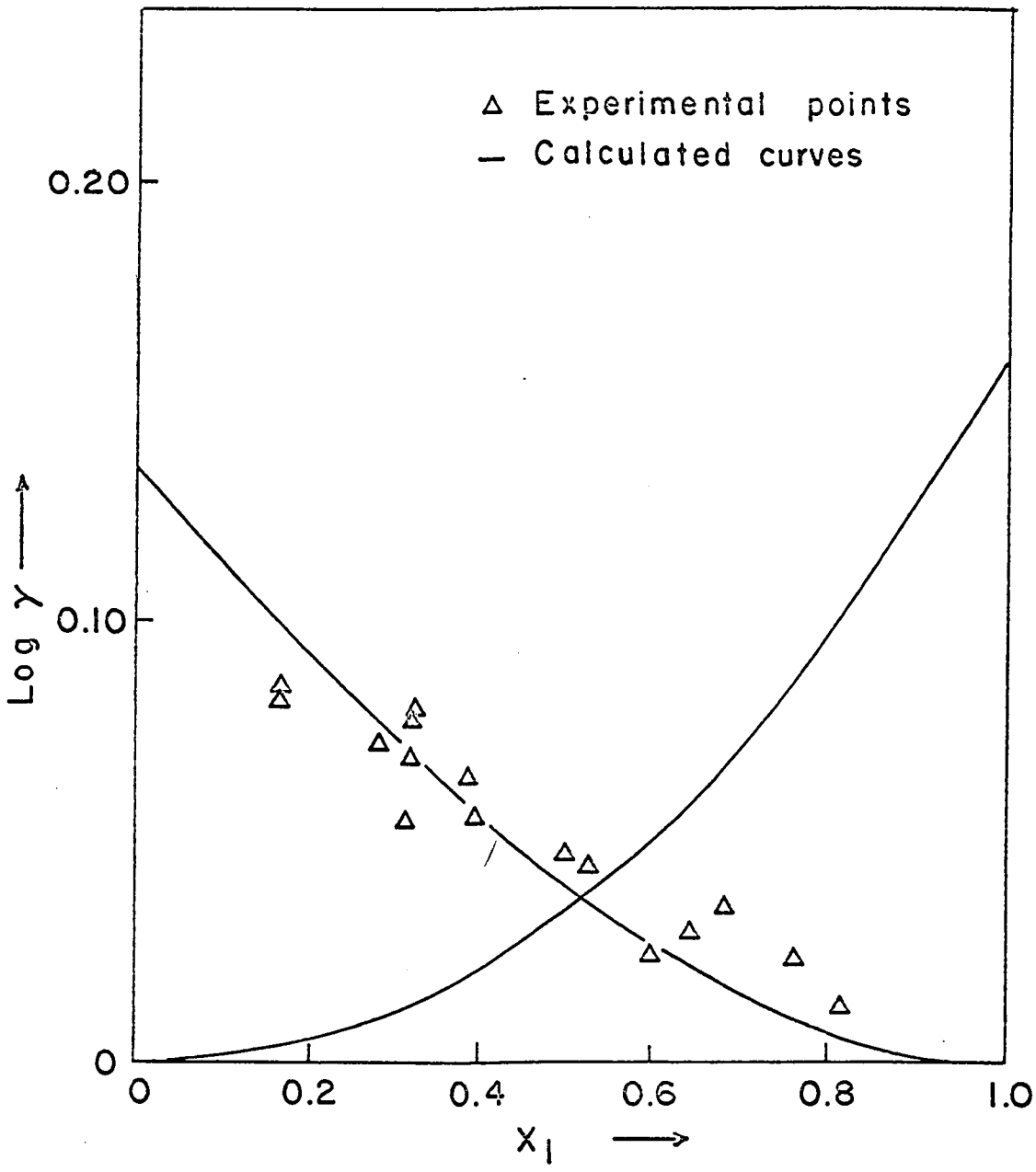

Log γ vs x_1 at 132.52 °K

Fig. 17

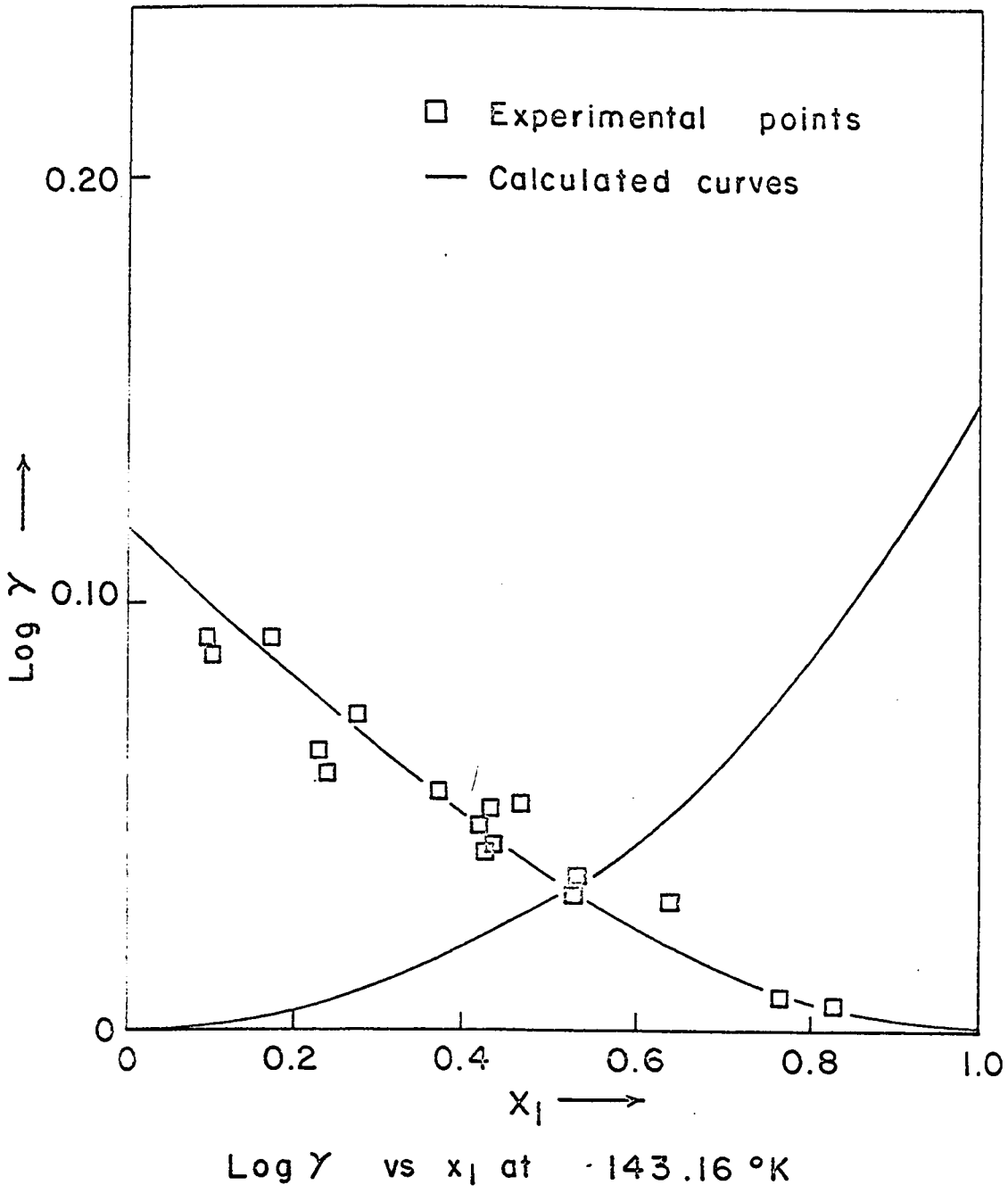
Experimental points
Calculated curves
0.20
0.10
0
Log γ
0
0.2
0.4
0.6
0.8
1.0
X_1
Log γ vs x_1 at 143.16 °K

Fig. 18

LIQUID PHASE FUGACITY COEFFICIENT OF PURE METHANE

The liquid phase fugacity coefficients were calculated from experimental values based on the equation:

$$\hat{\phi}_i^{\circ} = \frac{y_i}{x_i} \frac{\hat{\phi}_i^{V}}{\gamma_i^{L}}$$

in which y_i and x_i were the experimentally determined equilibrium compositions. $\hat{\phi}_i^{V}$'s were calculated based on the Redlich-Kwong equation of state (27). The activity coefficients were calculated using the two constant Redlich-Kister equations as stated before.

The liquid phase activity coefficients for pure methane were plotted against the reduced pressure on a log-log scale in Figure 19. The values are tabulated in Tables 8, 9 and 10 in Appendix V.

The $\hat{\phi}_i^{\circ}$ values are compared with the calculated values based on the data of Mathews and Hurd (19) at saturation in Appendix V. The agreement of the values is within $\pm$ 6%.

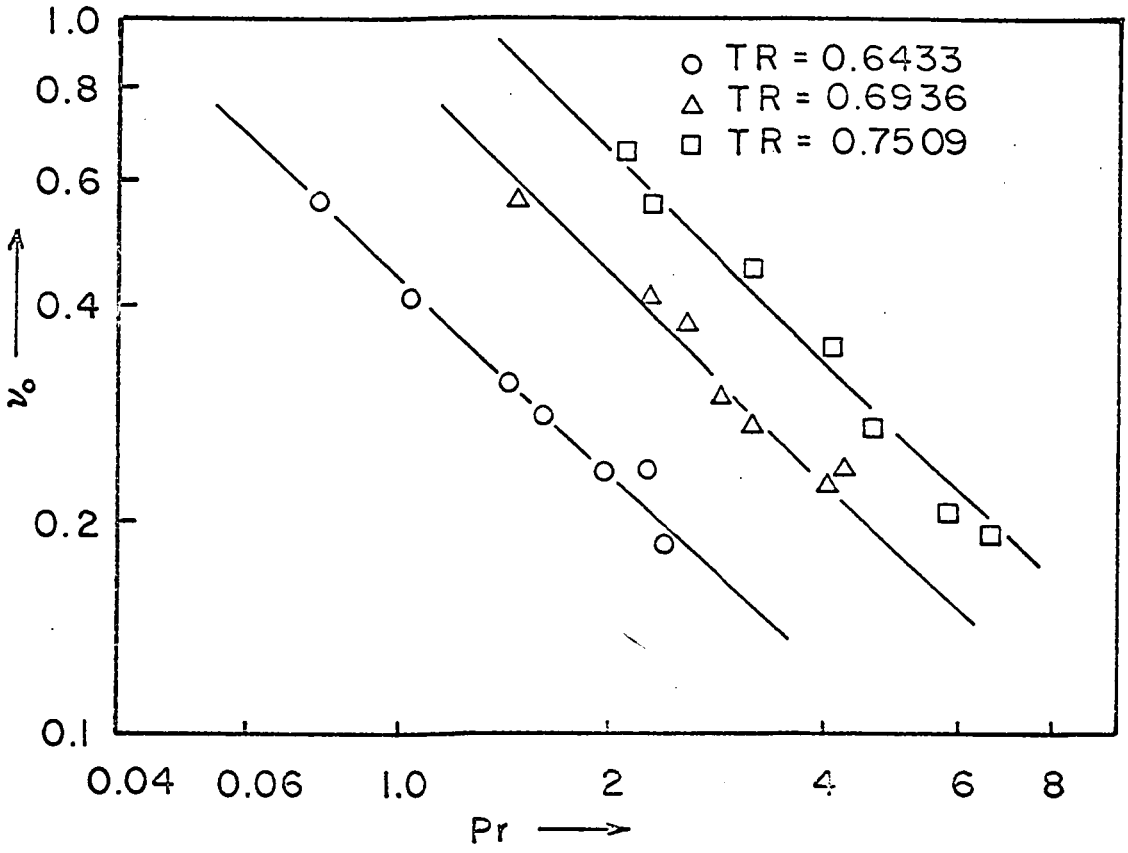

Fugacity coefficient of pure methane (liquid) vs. reduced pressure

Fig. 19

DISCUSSIONS AND CONCLUSIONS

The following are the comments on the observations.

The equipment:

The forced circulation type equipment, which was built and used in the present experimental work was a versatile one. It was suitable for measurements of total pressure and vapour liquid equilibria studies for two phase multicomponent systems for a wide range of temperature. The obtained data were reproducible.

The results and calculated values:

The working temperature and pressure were chosen below the critical temperature of both the components and the mixtures (17). The temperature and pressure ranges were as follows:

Isotherm	Temperature °K	Pressure range psia
I	122.66	34 - 205
II	132.52	60 - 340
III	143.16	106 - 520

The three sets of isothermal data are suitable for extrapolation and also for calculation of the effect of temperature and pressure on composition.

A Gibbs-Duhem area test for the consistency of the data is not possible due to the unavailability of reliable pure component liquid phase fugacity coefficient for methane.

The argon-methane mixtures at this temperature range are not too far from ideal. The excess Gibbs free energy of mixing is less than 30 calories per gram mole.

Two constant Redlich-Kwong equation was used for correlation.

The constant of the equations obtained are:

Temperature °K	B	C
122.66	0.18434	0.01521
132.52	0.14597	0.01315
143.16	0.13652	0.01282

The excess Gibbs free energies for 50 mole % liquid mixture are as follows:

Temperature °K	G^E cal/g mole
122.66	25.503
132.52	22.247
143.16	21.495

The values are slightly higher than the extrapolated values of Sprow and Prausnitz (37), but closer to the extrapolated values of Mathot (47).

The x - y plots in Figure 13 show that the x - y curves approach the diagonal as the temperature rises. The activity coefficients for both the gases decrease with rise in temperature.

The fugacity coefficient in the liquid phase for pure methane:

A set of fugacity coefficient values of pure methane were calculated from the experimental data. These values differ from those predicted based on Pitzer's data at saturation for zero accentric factor. The experimental values are useful for future calculations and suitable for extrapolation and intrapolation. The agreement of the values with those of Mathews and Hurd (19) is within $\pm$ 6%.

The prediction methods:

The theory based on the creation of cavity in the solvent for the solute molecule and the interaction between the solvent and the solute molecules is discussed in Appendix VI.

In this method the problem was encountered mainly in the calculation of the interaction energy between solvent and solute mole-

cules. The interaction energies at different temperature are calculated from Lennerd-Jones model assuming the radial distribution function equal to unity. The interaction energies are also calculated from other functions including the experimental values, i.e., G_e/RT, $\ln (RT/V)$ and $\ln (f_2/x_2)$. The values of $(\overline{G}_i/RT)_{solute}$ $(\rho_{solvent}/T)$ are compared. According to the Lennerd-Jones model with radial distribution function equal to unity $(\overline{G}_i/RT)_{solute}/(\rho_{solvent}/T)$ should be constant for a binary system. But the comparison shows that they are not constant. Further, the values for argon and methane are different.

It may be concluded that the radial distribution function is not equal to unity and is also a function of temperature (or density) and the shape of the molecules. Further calculations with different molecules will help in finding out the functions.

Appendix I

Tables of Experimental Data

Table 1

T = 122.66°K

No.	Pressure psig	y_1	x_1
1	118.0	0.855	0.565
2	109.0	0.835	0.325
3	178.0	0.9673	0.924
4	104.5	0.829	0.520
5	130.0	0.894	0.638
6	146.5	0.922	0.744
7	95.0	0.795	0.418
8	136.5	0.882	0.680
9	126.0	0.848	0.594
10	113.0	0.850	0.537
11	103.5	0.798	0.457
12	86.0	0.720	0.3585
13	82.0	0.750	0.342
14	70.5	0.698	0.263
15	55.0	0.611	0.199
16	54.5	0.624	0.1895
17	36.5	0.447	0.098
18	68.0	0.688	0.25
19	183.0	0.972	0.966
20	51.5	0.592	0.177
21	132.5	0.907	0.662
22	177.5	0.962	0.92
23	90.0	0.795	0.398

Table 2

T = 132.52°K

No.	Pressure psig	y_1	x_1
1	273.0	0.914	0.813
2	255.0	0.913	0.776
3	124.5	0.597	0.272
4	138.0	0.6465	0.3125
5	157.0	0.6965	0.3930
6	137.0	0.638	0.317
7	112.0	0.5725	0.265
8	84.0	0.4605	0.1605
9	67.0	0.2942	0.095
10	87.0	0.4616	0.1675
11	233.5	0.8655	0.654
12	189.0	0.790	0.505
13	141.0	0.6555	0.3205
14	154.5	0.697	0.3785
15	132.5	0.626	0.310
16	237.5	0.833	0.689
17	257.0	0.905	0.766
18	174.0	0.774	0.438
19	215.0	0.832	0.600
20	233.0	0.858	0.647
21	194.0	0.854	0.537

Table 3

T = 143.16°K

No.	Pressure	y_1	x_1
1	257.0	0.7095	0.4325
2	431.0	0.9295	0.8295
3	346.0	0.887	0.613
4	321.5	0.835	0.560
5	268.5	0.7155	0.433
6	259.0	0.708	0.427
7	197.5	0.5785	0.275
8	284.0	0.7438	0.470
9	271.5	0.7295	0.440
10	223.5	0.6555	0.372
11	175.5	0.5095	0.2425
12	126.0	0.3115	0.0982
13	129.0	0.3142	0.1015
14	208.0	0.574	0.2978
15	189.5	0.5595	0.274
16	313.0	0.838	0.536
17	357.0	0.842	0.640
18	311.0	0.802	0.530
19	395.0	0.895	0.752
20	152.5	0.475	0.208
21	267.0	0.718	0.435
22	198.0	0.57	0.273
23	166.0	0.542	0.230
24	151.0	0.502	0.171
25	306.0	0.843	0.555

Appendix II

The Quality of Gases

Argon gas was supplied by Union Carbide Canada Ltd., Linde Gases Division, Ottawa-1. The typical analysis supplied by the manufacturer is as follows:

Purity (minimum)	99.996%
Moisture	6 ppm
Oxygen - less than	1 ppm
Hydrogen - less than	1 ppm
Carbon bearing compounds - less than	3.3 ppm
Nitrogen - less than	2.6 ppm
Group V compounds (as PH_3) - less than	4 ppm

Methane gas was supplied by Matheson of Canada Ltd., Whitby, Ontario. A typical analysis of the research grade methane used:

Purity	99.90%
CO_2	40 - 50 ppm
N_2	19.8 ppm
C_2H_4 - less than	10 ppm
C_3H_8 - less than	5 ppm

The chromatographic analysis did not show the traces of impurities present mentioned above.

Appendix III

Calibration of Measuring Devices

The calibration of thermocouples:

The copper constantan thermocouples were supplied by the Thermo Electric Company. A calibration chart for the thermocouple was obtained. The chart showed the millivoltage against temperature. The different points in the chart were verified by measuring the melting point of ice and the vapour pressure of argon at different temperatures.

The reference junction was placed in an ice bath, the temperature of which was measured by a precision thermometer.

The vapour pressure of argon at different temperatures are shown and compared below:

		Vapour Pressure	
-m V	T°C	Expti. atm. abs.	Literature (22) atm. abs.
4.615	-150.5	13.78	13.80
4.377	-140.0	23.22	23.20
4.136	-129.9	35.60	35.50

The values obtained above are in very close resemblance to each other and well within experimental error.

The millivolt vs the temperature curve is shown in Figure 20.

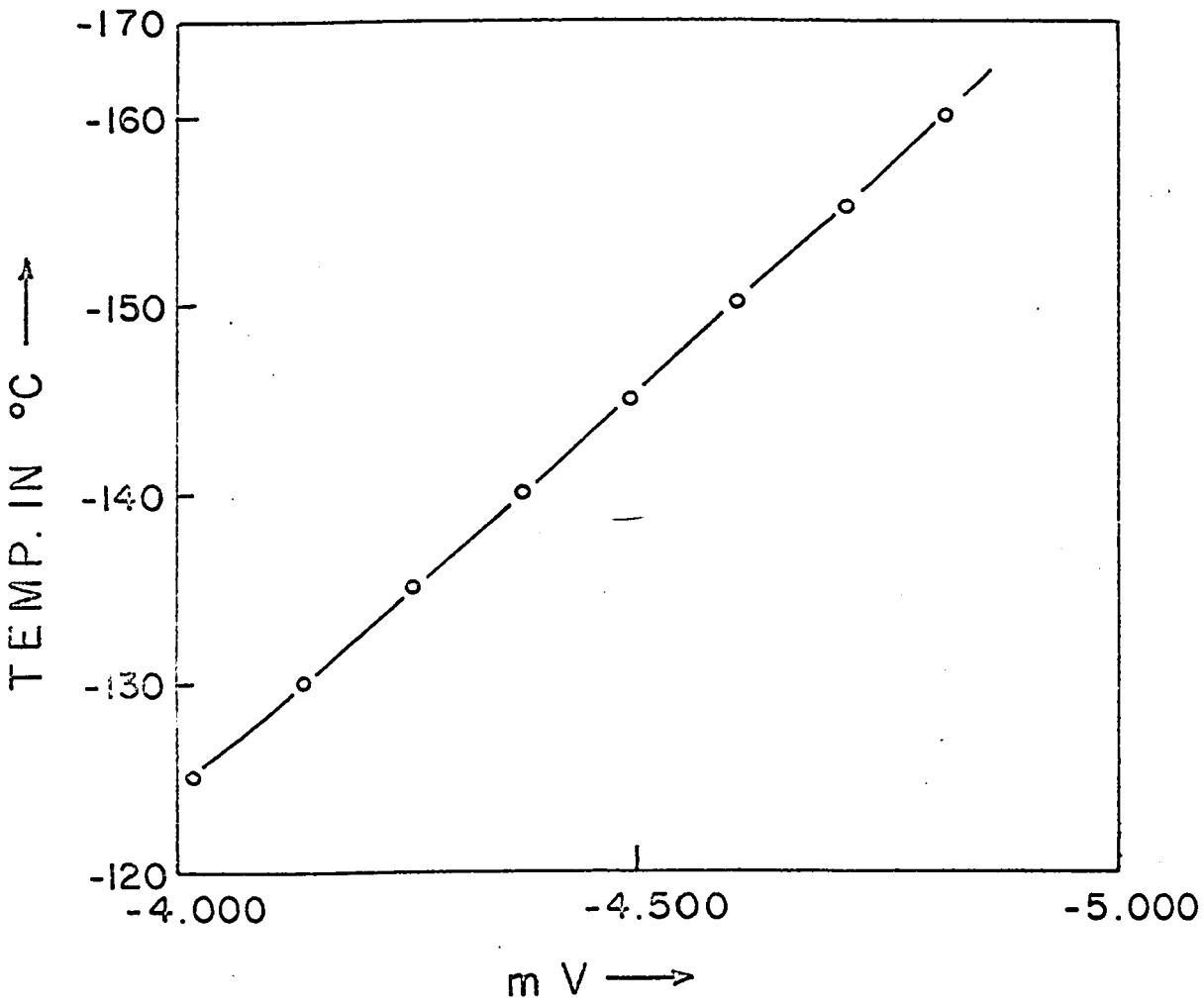

Calibration curve for copper-constanstan thermocouple

Fig. 20

Calibration of the pressure gauge:

The pressure in the experiments varied from 15 to 510 psig, and was measured with the test pressure gauge range: 0 - 600 psig, with 2 psi divisions. The pressure gauge was calibrated using a dead weight tester at the Division of Fuels and Mining Practice, High Pressure Chemistry Section, Mines and Technical Department, Government of Canada. The report No. 66083 is tabulated in Table 4.

Calibration of the chromatograph:

The chromatograph was calibrated with prepared samples of known compositions. The retention time was slightly above two minutes. The peaks were separate. A typical chart diagram is shown in Figure 6. The area was measured using an integrator as well as by measuring the area of the triangle formed. Wagner and Weber (44) have suggested a plot of mole fraction ratio vs peak area ratio. This was further modified by Deshpande and Lu (8). In this case the mole fraction ratio was plotted against peak area ratio (Fig. 21).

The reproducibility was within $\pm$ 0.2 mole % in the range of 20 to 80 mole % composition.

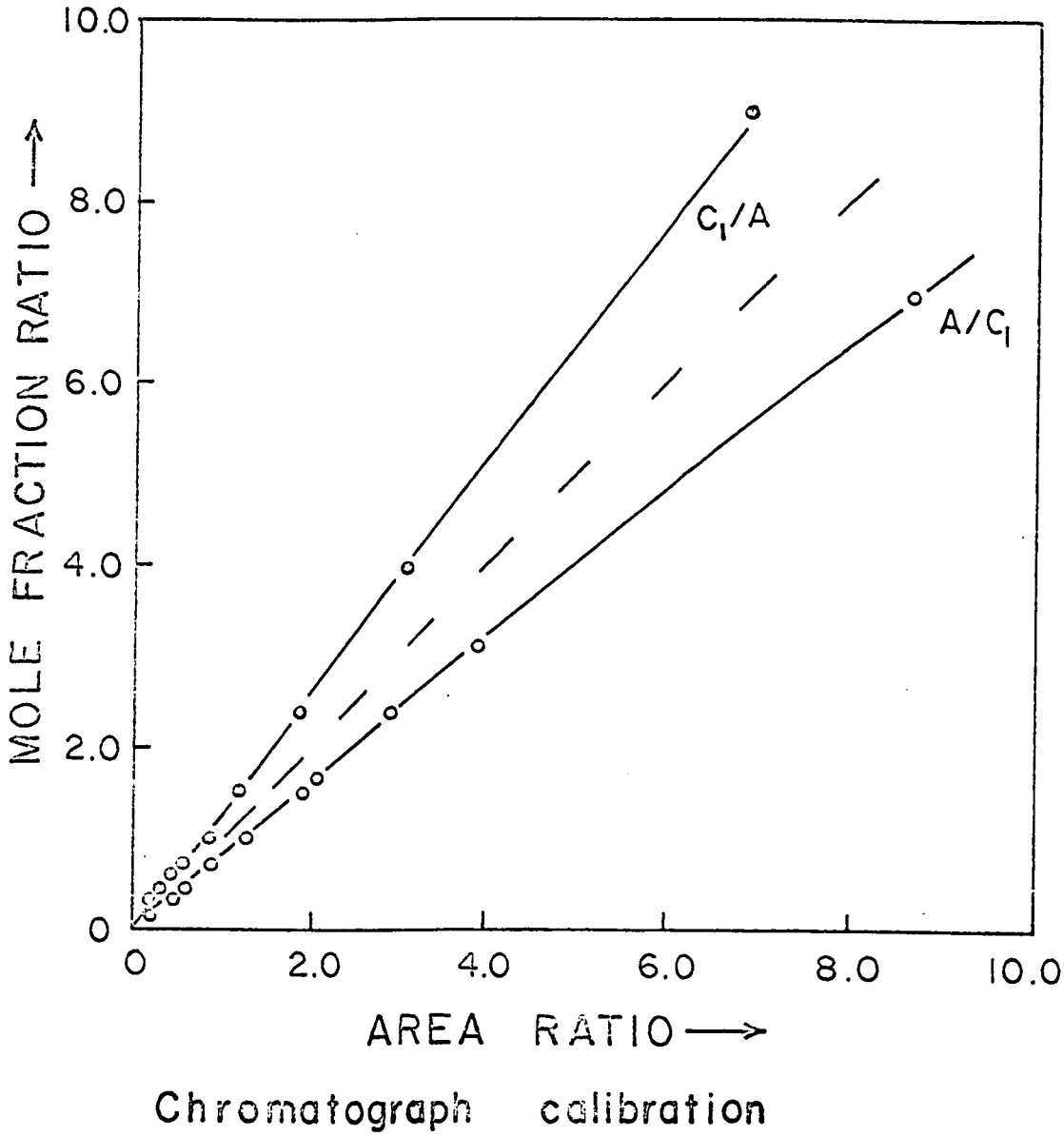
10.0
8.0
6.0
4.0
2.0
0
MOLE FRACTION RATIO ⟶
C_1/A
A/C_1
0
2.0
4.0
6.0
8.0
10.0
AREA RATIO ⟶
Chromatograph calibration

Fig. 21

Table 4

True Pressure psig	Gauge Pressure psig	Deviation psi
0	0	0
5	4.5	-0.5
10	8.5	-1.5
15	14.0	-1.0
20	18.5	-1.5
25	23.5	-1.5
30	28.0	-2.0
35	33.5	-1.5
40	38.5	-1.5
45	43.0	-2.0
50	49.0	-1.0
55	54.0	-1.0
60	58.5	-1.5
65	63.0	-2.0
70	68.0	-2.0
75	73.0	-2.0
80.0	78.0	-2.0
85.0	83.0	-2.0
90.0	88.0	-2.0
95.0	94.0	-1.0
100.0	98.0	-2.0
105.0	103.0	-2.0
110.0	108.0	-2.0
115.0	113.0	-2.0

Table 4 (Continued)

True Pressure psig	Gauge Pressure psig	Deviation psi
120.0	118.0	-2.0
125.0	122.5	-2.5
130.0	128.0	-2.0
135.0	132.5	-2.5
140.0	137.5	-2.5
145.0	142.5	-2.5
150.0	147.5	-2.5
155.0	152.5	-2.5
160.0	157.0	-3.0
165.0	162.0	-3.0
170.0	167.0	-3.0
175.0	172.0	-3.0
180.0	177.0	-3.0
185.0	182.0	-3.0
190.0	187.0	-3.0
195.0	192.0	-3.0
200.0	197.0	-3.0
205.0	202.0	-3.0
210.0	207.0	-3.0
215.0	212.0	-3.0
220.0	217.0	-3.0
225.0	221.5	-3.5
230.0	226.5	-3.5
235.0	231.5	-3.5

Table 4 (Continued)

True Pressure psig	Gauge Pressure psig	Deviation psi
240.0	236.5	-3.5
245.0	241.5	-3.5
250.0	247.0	-3.0
255.0	252.0	-3.0
260.0	257.0	-3.0
265.0	262.0	-3.0
270.0	267.0	-3.0
275.0	272.0	-3.0
280.0	277.0	-3.0
285.0	282.0	-3.0
290.0	287.0	-3.0
300.0	297.0	-3.0
305.0	302.0	-3.0
310.0	307.0	-3.0
315.0	311.5	-3.5
320.0	316.5	-3.5
325.0	321.5	-3.5
330.0	326.5	-3.5
335.0	331.5	-3.5
340.0	336.5	-3.5
345.0	342.0	-3.0
350.0	347.0	-3.0
355.0	352.0	-3.0
360.0	357.0	-3.0

Table 4 (Continued)

True Pressure psig	Gauge Pressure psig	Deviation psi
365.0	362.0	-3.0
370.0	367.0	-3.0
375.0	372.0	-3.0
380.0	377.0	-3.0
385.0	382.0	-3.0
390.0	387.0	-3.0
395.0	392.0	-3.0
400.0	397.0	-3.0
405.0	402.0	-3.0
410.0	407.0	-3.0
420.0	417.0	-3.0
425.0	422.0	-3.0
430.0	427.0	-3.0
435.0	432.0	-3.0
440.0	437.0	-3.0
445.0	442.0	-3.0
450.0	447.0	-3.0
455.0	452.0	-3.0
460.0	457.0	-3.0
465.0	462.0	-3.0
470.0	467.0	-3.0
475.0	472.0	-3.0
480.0	477.0	-3.0
485.0	482.0	-3.0

Table 4 (Continued)

True Pressure psig	Gauge Pressure psig	Deviation psi
490.0	487.0	-3.0
495.0	492.0	-3.0
500.0	497.0	-3.0
505.0	502.0	-3.0
510.0	507.0	-3.0
515.0	511.5	-3.5
520.0	516.5	-3.5
525.0	521.5	-3.5
530.0	526.5	-3.5
535.0	531.5	-3.5
540.0	536.5	-3.5
545.0	541.5	-3.5
550.0	546.5	-3.5
525.0	522.0	-3.0
500.0	497.0	-3.0
475.0	472.0	-3.0
450.0	447.0	-3.0
425.0	422.5	-2.5
400.0	397.5	-2.5
375.0	372.0	-3.0
350.0	347.0	-3.0
325.0	322.0	-3.0
300.0	297.0	-3.0
275.0	272.0	-3.0
250.0	247.0	-3.0

Table 4 (Continued)

True Pressure psig	Gauge Pressure psig	Deviation psi
225.0	222.0	-3.0
200.0	197.5	-2.5
175.0	172.0	-3.0
150.0	148.0	-2.0
125.0	123.0	-2.0
100.0	98.5	-1.5
75.0	74.0	-1.0
50.0	49.0	-1.0
25.0	24.0	-1.0

Appendix IV

Activity Coefficient of Argon in the Mixture

Table 5

$T = 122.66°K$ $\quad f^{\circ} = 11.4084$ atm

No.	x_1	(y_1/x_1)	P atm	$\hat{\phi}_1$	log γ_1	log γ_1/x_2^2
1	0.565	1.51330	9.023	0.8871	0.03310	0.1749
2	0.525	1.59050	8.4169	0.8949	0.02925	0.1296
3	0.924	1.04690	13.1121	0.8366	0.00389	0.6735
4	0.52	1.59420	8.1107	0.8995	0.01681	0.0729
5	0.638	1.40125	9.8459	0.8764	0.03113	0.2376
6	0.744	1.23924	10.9681	0.8623	0.01592	0.2426
7	0.418	1.90191	7.4663	0.9071	0.06213	0.1834
8	0.537	1.58290	8.6891	0.8921	0.03919	0.1828
9	0.457	1.7462	8.0426	0.9085	0.05718	0.1939
10	0.342	2.1920	6.5797	0.9184	0.07578	0.1750
11	0.263	2.6540	5.7971	0.9288	0.10974	0.2020
12	0.199	3.07040	4.7425	0.9420	0.09351	0.1457
13	0.1895	3.29287	4.7084	0.9421	0.12085	0.1839
14	0.098	4.56122	3.4836	0.9589	0.14076	0.1730
15	0.25	2.6980	5.6301	0.9309	0.10499	0.1867

Table 5 (Continued)

$T = 122.66°K$ $\quad f° = 11.4084$ atm

No.	x_1	(y_1/x_1)	P atm	ϕ_1	log γ_1	log γ_1/x_2^2
16	0.177	3.3446	4.5044	0.9447	0.10989	0.1622
17	0.662	1.37010	10.0161	0.8754	0.02807	0.2457
18	0.92	1.04565	13.0781	0.8370	0.00240	0.3750
19	0.398	1.9975	7.1241	0.9120	0.06594	0.18195
20	0.680	1.2971	10.2882	0.8723	0.02423	0.2366
21	0.594	1.4276	9.5737	0.8828	0.04051	0.2457
22	0.3585	2.0084	6.8518	0.9145	0.07372	0.1791
23	0.966	1.00621	13.4524	0.8315	$\bar{1}.99930$	-

Table 6

$T = 132.52\,^{\circ}K$ $f^{\circ} = 16.796$ atm

No.	x_1	y_1/x_1	P atm	$\hat{\phi}_1$	$\log \gamma_1$	$\log \gamma_1/x_2^2$
1	0.813	1.1242	19.5765	0.7813	0.01248	0.3570
2	0.776	1.176	18.3517	0.8124	0.02273	0.4530
3	0.272	2.1949	9.4717	0.9130	0.07084	0.1329
4	0.3125	2.0688	10.3903	0.8993	0.0773	0.1635
5	0.3930	1.7723	11.6832	0.8906	0.05495	0.1491
6	0.3170	2.0126	10.3223	0.8995	0.06757	0.1448
7	0.265	2.16037	8.6211	0.9201	0.0270	0.0705
8	0.1605	2.8692	7.305	0.9361	0.08051	0.1147
9	0.095	3.0968	5.5591	0.9508	0.0112	0.0137
10	0.1675	2.7558	7.506	0.9360	0.08244	0.11895
11	0.654	1.3234	16.6887	0.8203	0.03958	0.3306
12	0.505	1.56435	13.1802	0.8700	0.04064	0.1659
13	0.3205	2.0452	10.5944	0.8954	0.07861	0.1703
14	0.3785	1.8415	11.5131	0.8863	0.06228	0.1612
15	0.310	2.0194	10.0161	0.9052	0.05436	0.1149

Table 6 (Continued)

T = 132.52° K f° = 16.796 atm

No.	x_1	$\gamma_1 x_1$	P atm	$\hat{\phi}_1$	log γ_1	log γ_1/x_2^2
16	0.689	1.28156	17.0609	0.8210	0.03501	0.3619
17	0.766	1.18146	18.4878	0.8107	0.02689	0.4911
18	0.600	1.3867	14.62983	0.8533	0.02295	0.1434
19	0.647	1.3261	15.8503	0.8397	0.02951	0.2368
20	0.537	1.5903	13.1972	0.8595	0.04304	0.2008
21	0.438	1.6712	11.8399	0.8820	0.02177	0.0689

Table 7

$T = 143.16°K$ $\quad f^{\circ} = 34.9098$ atm

No.	x_1	y_1/x_1	P atm	$\hat{\phi}_1$	log γ_1	log γ_1/x_2^2
1	0.4325	1.6405	18.4878	0.8530	0.04144	0.1287
2	0.8295	1.12055	30.3277	0.7350	0.00619	0.2129
3	0.433	1.6524	19.2703	0.8479	0.0582	0.1810
4	0.427	1.6581	18.6238	0.8504	0.04779	0.1455
5	0.470	1.5826	20.3250	0.8392	0.05379	0.1915
6	0.440	1.6580	19.4744	0.8418	0.06123	0.1952
7	0.372	1.7621	17.2082	0.8737	0.05559	0.1409
8	0.435	1.6500	19.3620	0.8498	0.06166	0.1916
9	0.2425	2.10103	13.942	0.9009	0.05944	0.1036
10	0.1205	2.4400	9.3016	0.9340		
11	0.2978	1.9275	15.1535	0.8830	0.0457	0.0927
12	0.274	2.042	13.8947	0.8932	0.04028	0.0764
13	0.54	1.4167	21.9581	0.8299	0.03466	0.1638
14	0.64	1.3156	25.0923	0.7831	0.0295	0.2281
15	0.536	1.5132	20.5622	0.8304	0.0304	0.1739

Table 7 (Continued)

T = 143.16° K f° = 34.9098 atm

No.	x_1	y_1/x_1	P atm	$\hat{\phi}_1$	log γ_1	log γ_1/x_2^2
16	0.752	1.19015	26.8781	0.7736	0.00798	0.1297
17	0.208	2.28365	10.377	0.9280		
18	0.435	1.650	18.1682	0.8594	0.0414	0.1297
19	0.273	2.0879	14.6930	0.89407	0.0732	0.1385
20	0.230	2.3565	12.2925	0.9148	0.06399	0.1079
21	0.171	2.9356	10.3424	0.9248	0.09073	0.1320
22	0.555	1.5189	20.8367	0.8265	0.04058	0.2049
23	0.275	2.1036	14.4390	0.8941	0.06889	0.1311
24	0.098	3.1721	9.5738	0.9310	0.09006	0.11069
25	0.1015	3.0956	9.7779	0.9293	0.08680	0.1075

Appendix V

Calculation of Liquid Phase Fugacity Coefficient for Methane

Table 8

$T = 122.66°K$ $T_R = 0.6633$

No.	x_1	y_2/x_2	$\hat{\phi}_2$	Y_2	ω_2	P_{R_2}
1	0.565	0.3333	0.7923	1.1338	0.2329	0.1971
2	0.680	0.36875	0.7648	1.2082	0.2334	0.2246
3	0.744	0.30468	0.7512	1.2601	0.1816	0.2395
4	0.418	0.35223	0.8255	1.0672	0.2725	0.1630
5	0.342	0.37993	0.8444	1.0434	0.3074	0.1437
6	0.1895	0.46391	0.8871	1.0124	0.4065	0.1028
7	0.098	0.61308	0.9147	1.0032	0.5590	0.0761

The ω_o values calculated based on the data of Mathews and Hurd at saturation.

1	0.2377	5	0.3265
2	0.2283	6	0.4369
3	0.2004	7	0.6084
4	0.2876		

Table 9

$T = 132.52°K$ $\quad T_R = 0.6936$

No.	x_1	y_2/x_2	$\hat{\phi}_2$	γ_2	σ_2	P_{R_2}
1	0.813	0.4599	0.6422	1.2569	0.2349	0.4274
2	0.393	0.5000	0.7730	1.0462	0.3694	0.2551
3	0.317	0.5300	0.7979	1.0388	0.4071	0.2254
4	0.1605	0.6426	0.8656	1.0068	0.5525	0.1466
5	0.505	0.4242	0.7508	1.0814	0.2945	0.2878
6	0.766	0.4060	0.6654	1.2207	0.2213	0.4037
7	0.600	0.4200	0.7285	1.1217	0.2728	0.3194

The σ_o values calculated based on the data of Mathews and Hurd at saturation.

1	0.2203	5	0.3057
2	0.3481	6	0.2218
3	0.3852	7	0.2772
4	0.5370		

Table 10

$T = 143.16°K$ $\quad T_R = 0.7509$

No.	x_1	y_2/x_2	$\hat{\phi}_2$	γ_2	ϕ_2	P_{R_2}
1	0.4325	0.5119	0.7143	1.0505	0.3481	0.4037
2	0.8295	0.4135	0.5650	1.2394	0.1885	0.6622
3	0.275	0.5814	0.7720	1.0186	0.4406	0.3153
4	0.0982	0.7635	0.8439	1.0021	0.6430	0.2090
5	0.530	0.4213	0.6809	1.0804	0.2655	0.4621
6	0.752	0.4234	0.5686	1.1865	0.2029	0.5869
7	0.208	0.6629	0.8317	1.0130	0.5443	0.2266

The ϕ values calculated based on the data of Mathews and Hurd at saturation.

1	0.3655	5	0.2756
2	0.2090	6	0.2129
3	0.4310	7	0.5440
4	0.6130		

Appendix VI

Calculations Based on Molecular Theory

Prediction based on molecular theory:

The problem of solubility at infinite dilution is at present looked upon as a two stage operation. A cavity is created for the solute molecule in the solvent and then the solute molecule is placed in the solvent. The creation of the cavity would require energy termed as "the energy of cavitation". The solute molecule when placed inside the solvent would interact with the solvent molecules. The energy encountered is termed as "energy of interaction".

This theory was proposed first by Uhlig (42) and Eley (11), but has not been utilised for a long time. Pioretti (20) calculated some values of Henry's law constants, which showed large differences with the experimental results.

The chemical potential (13) in the liquid phase for the solvent molecule is given by the following equation:

$$\mu_2^L = -\chi_2 + P\bar{v}_2 - kT \ln \lambda_2^3 j_2 + kT \ln \left(\frac{N_2}{V}\right) \qquad \text{VI-1}$$

where $-\chi_2$ is the potential energy of the solute molecule in the solution relative to infinite separation. $P\bar{v}_2$ is the pressure-volume energy of the solute molecules. $V\lambda_2^3$ and j_2 are the partition functions per molecule for the translational and internal degrees of freedom for solute.

The subscript 1 stands for the solvent and subscript 2 stands for the solute.

For a very dilute solution $\frac{N_2}{N_1}$ is approximately equal to x_2

and $$V = N_1 v_1 \qquad \text{VI - 2}$$

then $$\frac{N_2}{V} = x_2/v_1 \qquad \text{VI - 3}$$

Considering the solution to be very dilute, the solute-solute interaction can be neglected.

The $(-\chi_2 + P\bar{v}_2)$ may be replaced by $(\bar{g}_c + \bar{g}_1)$, where $\bar{g}_c$ represents the partial molecular Gibbs free energy required to create a site in the solvent for a rigid sphere having the same size as the solute molecule and $\bar{g}_1$ is the partial molecular Gibbs free energy of interaction between the solvent molecule and the solute molecule . This is identical to that of charging the hard sphere or cavity introduced in the first case to the required potential.

So,

$$\mu_2^L = \bar{g}_1 + \bar{g}_c - kT \ln (\lambda_2^3 j_2) + kT \ln (x_2/v_1) \qquad \text{VI - 4}$$

The chemical potential in the vapour phase of the solute is given by the following equation:

$$\mu_2^V = -kT \ln (\lambda_2^3 j_2) + kT \ln \bar{f}_2/kT \qquad \text{VI - 5}$$

Pioretti used pressure instead of fugacity.

At equilibrium,

$$\mu_2^L = \mu_2^V \qquad \text{VI-6}$$

Substituting for μ_2^L and μ_2^V

$$\bar{g}_c + \bar{g}_i + kT \ln (x_2/v_1) = kT \ln (\bar{f}_2/kT) \qquad \text{VI-7}$$

Rearranging,

$$kT \ln \frac{\bar{f}_2}{x_2} = \bar{g}_i + \bar{g}_c + kT \ln \left(\frac{kT}{v_1}\right) \qquad \text{VI-8}$$

Multiplying both sides by $\tilde{N}$ the Avogadro's number, and then dividing both sides by $\tilde{N}kT = RT$

$$\ln \frac{\bar{f}_2}{x_2} = \frac{\bar{G}_i}{RT} + \frac{\bar{G}_c}{RT} + \ln \left(\frac{RT}{V_1}\right) \qquad \text{VI-9}$$

where $\bar{G}_i$, $\bar{G}_c$ and V_1 represent the partial molal and molal properties.

The partial molal Gibbs free energy of creating a cavity in a fluid of hard spheres is given by Reiss and coworkers (32, 33), as:

$$\bar{G}_c = K_o + K_1 a_{12} + K_2 a_{12} + K_3 a_{12}^3 \qquad \text{VI-10}$$

where

$$K_o = RT \left[-\ln (1-y) + 9/2 \{ y/(1-y) \}^2 \right] - \frac{\pi P a_1^3}{6} \qquad \text{VI-11}$$

$$K_1 = -\frac{RT}{a_1}\left[6y/(1-y) + 18\left\{y/(1-y)\right\}^2\right] + \pi P a_1^2 \qquad \text{VI-12}$$

$$K_2 = \frac{RT}{a_1^2}\left[12y/(1-y) + 18\left\{y/(1-y)\right\}^2\right] - 2\pi P a_1 \qquad \text{VI-13}$$

where,

$$y = (\pi a_1^3 \rho)/6 \qquad \text{VI-14}$$

$$a_{12} = (a_1 + a_2)/2 \quad = K_3 = \frac{4}{3}\pi RTP$$

The partial molal Gibbs free energy of interaction is given as

$$\bar{G}_i = \bar{E}_i + P\bar{V} - T\bar{S}_i \qquad \text{VI-15}$$

$P\bar{V}$ is very small in comparison with $\bar{E}_i$ and also for non polar (simple) molecules $\bar{S}_i$ is negligible. Therefore

$$\bar{G}_i = \bar{E}_i \qquad \text{VI-16}$$

The interaction energy of a non polar solute molecule with non polar solvent molecules can be calculated from various empirical equations proposed. But the difficulty in obtaining a suitable expression for the radial distribution function in the liquid phase independent of the interaction energy, has limited the prediction of interaction energy.

Pioretti (20) assumed the radial distribution function as equal to one and calculated interaction energy between molecules based on Lennard-Jones (6 - 12) pairwise potential.

$$\bar{e}_i = c \sum_p (r_p^{-6} - {}_{12}^{6} r_p^{-12}) \qquad \text{VI-17}$$

where r_p is the distance between the solute and the P th solvent molecule. For the whole solvent replacing the summation by integration

$$\frac{\bar{e}_i(R)}{kT} = (4\pi\rho c/kT) \int_R^{\infty} (r^{-4} - {}_{12}^{6} r^{-10})\, dr \qquad \text{VI-18}$$

where R is the distance from the center of the solute molecule to the center of the nearest solvent molecule. The integration yields

$$\bar{e}_i(R)/kT = -(\epsilon^*/kT) \left[(2/R')^3 - \frac{8}{3} \left(\frac{1}{R'}\right)^9 \right] \qquad \text{VI-19}$$

where,

$$(\epsilon^*/kT) = \pi\rho c/(6kT\,\sigma_{12}^3) \qquad \text{VI-20}$$

$$c = 4(\epsilon_1 \epsilon_2)^{1/2} \sigma_{12}^6 \qquad \text{VI-21}$$

$$\sigma_{12} = (\sigma_1 + \sigma_2)/2 \qquad \text{VI-22}$$

and $$R' = R/\sigma_{12} \qquad \text{VI-23}$$

As σ_{12} is the distance of closest approach between solvent and solute molecules, R' is equal to unity. Then the equation reduces to

$$\bar{e}_1/kT = \frac{\bar{E}_1}{RT}$$

$$= \frac{\bar{G}_1}{RT}$$

$$= -5.33\,(\epsilon^*/kT) \qquad \text{VI - 24}$$

All the terms in the right hand side of equation VI - 9 may be evaluated as mentioned above. So the Henry's law constant

$$= \lim_{x \to 0} \frac{\bar{f}_2}{x_2} \qquad \text{VI - 25}$$

may be calculated.

At three temperatures the values of $\ln(\bar{f}_2/x_2)$, $\frac{\bar{G}_1}{RT}$, $\frac{\bar{G}_c}{RT}$ and $\ln(RT/V_1)$ are calculated based on the above mentioned equations.

Table 11

T° K	Component	$\ln(\bar{f}/x)$	$\bar{G}_c/RT$	$\bar{G}_1/RT$	$\ln(RT/V)$
122.66	A	2.86303	6.99728	-8.75016	5.54560
	CH_4	1.26850	6.15306	-9.86744	5.66577
132.52	A	3.23744	6.40840	-7.79164	5.58424
	CH_4	1.79523	5.12038	-8.29964	5.63441
143.16	A	3.58264	5.79155	-6.87989	5.61420
	CH_4	2.33440	3.78512	-6.44706	5.54926

Pieretti has shown that the values of $\overline{G}_c$ calculated as above are very accurate. So it seems that the discrepancies lie mainly in the values of $\overline{G}_i$. If $(\overline{G}_i/RT)$ is calculated from other functions $(\overline{G}_c/RT, \ln\frac{RT}{V}, \ln\frac{\overline{f}}{x})$ the following values are obtained.

	Component	122.66° K	132.52° K	143.16° K
(G_i/RT)	A	-9.65985	-8.75520	-7.82310
Based on other functions	CH_4	-10.55043	-8.95960	-6.9997
(G_i/RT)	A	-8.75016	-7.79164	-6.87989
Based on interaction	CH_4	-9.86744	-8.29964	-6.44706

The values differ very much. In the calculation of interaction energy the radial distribution function of the solvent is assumed to be unity. The shape of the molecules are assumed to be spherical. If the effect of the shape and radial distribution function is considered, the interaction energy may be represented as

$$\left(\frac{\overline{G}_i}{RT}\right)_{solute} = \frac{\rho_{solvent}}{T} \int u(r)\, g(r)\, f(b_1, b_2)$$

where, $u(r)$ is the energy of interaction based on the Lennard-Jones potential function.

$g(r)$ is the radial distribution function of the solvent (14, 18).

$f(b_1, b_2)$ is a function dependent on the shape of the solute (factor b_1) and the shape of the solvent (factor b_2) molecules.

The values of $(G_1/RT)_{solute}/(\frac{\rho_{solvent}}{T})$ are calculated, and the values are

T°K		122.66	132.52	143.16
$(G_1/RT)_{solute}/(\frac{\rho_{solvent}}{T}) \times 10^4$ based on experimental data	A	4.6566	4.7397	4.7945
	CH_4	4.5100	4.5530	4.5798
$(G_1/RT)_{solute}/(\frac{\rho_{solvent}}{T}) \times 10^4$ based on interaction (L. J. Potential)	A	4.22	4.22	4.22
	CH_4	4.22	4.22	4.22

From the above results it is clearly seen that the function $(G_1/RT)_{solute}/(\rho_{solvent}/T)$ is not constant for a binary system as postulated by the Pioretti model. The radial distribution function is dependent on temperature or in turn dependent on the molecular density. There should be a function involving the shape of the solvent and the solute molecules.

Appendix VII

Sample Calculations

Sample Calculations

1. Calculation of liquid phase fugacity coefficient of Argon:

Temperature: 122.66° K

v^L = 34.85 cc. g mole from Din's table (9)

$$\ln \varphi_\circ \left(\frac{P}{\varphi^\circ P^\circ}\right) = \frac{1}{RT} v^L (P - P^\circ)$$

or $$\log \varphi_\circ \left(\frac{P}{\varphi^\circ P^\circ}\right) = \frac{1}{2.303\,RT} v^L (P - P^\circ)$$

or $$\varphi_\circ = \frac{\varphi^\circ P^\circ}{P} \text{ antilog } \frac{v^L (P - P^\circ)}{2.303\,RT}$$

$\varphi^\circ P^\circ = f^\circ$ = 11.4085 atms., from Pitzer (46) values

P° = 13.8013 atms., from Din's tables

At P = 5 atms.

$(P - P^\circ)$ = -8.8013 atms.

$$\frac{v^L}{2.303\,RT} = \frac{34.85}{2.303 \times 82.06 \times 122.66} = 0.00149$$

$$\frac{v^L (P - P^\circ)}{2.303\,RT} = -0.013115$$

$$\frac{f^\circ}{P} = \frac{11.4085}{5} = 2.2817$$

$$\log \varphi_\circ \frac{P}{f^\circ} = -0.013115$$

or $$\log \frac{f^\circ}{\varphi_\circ P} = +0.03115$$

or $\frac{2.2817}{\rho} = 1.030$

or $\rho = \frac{2.2817}{1.0310} = 2.2152$

2. Chromatograph calibration:

Known sample:

$x_1 = 0.5$

$x_2 = 0.5$

$\frac{x_1}{x_2} = 1$

The area under the argon peak = 43941 (Integrater reading).

The area under the methane peak = 65070

$\frac{\text{area for Argon}}{\text{area for Methane}} = \frac{56070}{43941} = 1.273$

3. Calculation of composition from the calibrated curve:

Run no. 7, temperature = 122.66° K

The vapour phase

Area for Argon peak = 83383

Area for Methane peak = 17252

$\frac{\text{Area for Argon}}{\text{Area for Methane}} = 4.84$

From the calibration curve,

$$\frac{x_1}{x_2} = 3.88$$

$$x_2 = \frac{1}{4.88} = 0.205$$

$$x_1 = 1 - 0.205 = 0.795$$

4. Calculation of activity coefficient:

Run no. 7, temperature = 122.66° K

Pressure = 95.0 psig

= 7.4663 atms. abs.

Composition

$y_1 = 0.795$

$x_1 = 0.418$

critical temperature = 150.72° K

critical pressure = 48.0 atms. abs.

$T_R = 0.81382$

$P_R = 0.15554$

ϕ_1° from Figure 1 = 1.47

ϕ_1 in the vapour mixture calculated from Redlich-Kwong equation of state using the IBM 1620 computer = 0.90705.

Therefore

$$\gamma_1 = \frac{0.795}{0.418} \times \frac{0.90705}{1.47} = 1.1712$$

$$\log \gamma_1 = 0.06865$$

5. Calculation of liquid phase fugacity coefficient for methane:

critical temperature of methane = 190.16° K

critical pressure of methane = 46.8 atm.

Temperature = 122.66° K

Pressure = 95 psig = 7.4663 atm. abs.

$T_R = 0.64334$

$P_R = 0.16301$

$y_2 = 1 - 0.795 = 0.205$

$x_2 = 1 - 0.418 = 0.582$

The fugacity coefficient in the mixture calculated from Redlich-Kwong equation of state using the IBM 1620 computer = 0.8255

The activity coefficient of methane is given by:

$$\log \gamma_2 = x_1^2 \left[B + C(x_1 - 3x_2) \right]$$
$$= x_1^2 \left[(B + C) - 4 C x_2 \right]$$

where $B = 0.18175$

$C = 0.01475$

Therefore,

$\log \gamma_2 = 0.02833$

$\gamma_2 = 1.0672$

$$\Phi = \frac{\gamma_2}{x_2} \times \frac{\phi_2}{\gamma_2}$$

$$= \frac{0.209}{0.582} \times \frac{0.8255}{1.0672}$$

$$= 0.2725$$

6. Calculation based on molecular theory:

Data:

at 122.66°K

From Din's table (9):

$v_2^L = 39.3$ cc/g mole

$v_1^L = 34.85$ cc/g mole

From Hirshfelder et al. (15):

$a_2 = 3.817 \times 10^{-8}$ cm

$a_1 = 3.405 \times 10^{-8}$ cm

$(\frac{\epsilon_i}{k})_2 = 148.2°K$

$(\frac{\epsilon_i}{k})_1 = 119.8°K$

$$a_{12} = \frac{a_1 + a_2}{2} = 3.611 \times 10^{-8} \text{ cm}$$

$$\left(\frac{\epsilon_i}{k}\right)_{12} = \sqrt{\left(\frac{\epsilon_i}{k}\right)_1 \left(\frac{\epsilon_i}{k}\right)_2} = \sqrt{119.8 \times 148.2} = 133.24°K$$

$$\rho_1 = \frac{1}{34.85} \times 6.023 \times 10^{23} \text{ molecules/cc}$$

$$= 0.028694 \times 6.023 \times 10^{23} \text{ molecules/cc}$$

$$\rho_2 = \frac{1}{39.3} \times 6.023 \times 10^{23} \text{ molecules/cc}$$

$$= 0.025445 \times 6.023 \times 10^{23} \text{ molecules/cc}$$

Calculation of $\frac{\overline{G}^e}{RT}$ for CH_4 solvent

$$y_2 = \frac{\pi}{6} \times \sigma_2^3 \rho$$

$$= \frac{\pi}{6} \times (3.405 \times 10^{-8})^3 \times 0.25445 \times 6.023 \times 10^{23}$$

$$= 0.44625$$

$$\frac{K_o}{RT} = \left[-\ln(1 - y_2) + \frac{9}{2}\left\{\frac{y_2}{1 - y_2}\right\}^2\right]$$

$$= \left[-\ln(1 - 0.44625) + \frac{9}{2}\left\{\frac{0.44625}{1 - 0.44625}\right\}^2\right]$$

$$= 3.51355$$

$$\frac{K_1 \sigma_2}{RT} = -\left[6\left(\frac{y_2}{1 - y_2}\right) + 18 \times \left(\frac{y_2}{1 - y_2}\right)^2\right]$$

$$= -\left[6 \times \left(\frac{0.44625}{1 - 0.44625}\right) + 18 \times \left(\frac{0.44625}{1 - 0.44625}\right)^2\right]$$

$$= -16.5253$$

$$\frac{K_2 a_2^2}{RT} = 12 \times \left(\frac{y_2}{1-y_2}\right) + 18 \times \left(\frac{y_2}{1-y_2}\right)^2$$

$$= 12 \times \left(\frac{0.44625}{1-0.44625}\right) + 18 \times \left(\frac{0.44625}{1-0.44625}\right)^2$$

$$= 21.36061$$

The terms $\frac{\Sigma P}{6} a_2^3$, $\Sigma P a_2^2$, $2\Sigma P a_2$ and $\frac{2}{3}\Sigma P a_{12}^3$ are neglected as these are of the order of 10^{-24}.

$$\frac{\bar{G}_e}{RT} = \frac{K_0}{RT} + \frac{K_1 a_{12}}{RT} + \frac{K_2 a_{12}^2}{RT} + \frac{K_3 a_{12}^3}{RT}$$

$$= 3.51355 - 16.5253 \left(\frac{3.611 \times 10^{-8}}{3.817 \times 10^{-8}}\right)$$

$$+ 21.36061 \left(\frac{3.611 \times 10^{-8}}{3.817 \times 10^{-8}}\right)^2 + 0$$

$$= 6.99728$$

$$\ln \frac{RT}{V^2} = 2.30257 \log \frac{82.06 \times 122.66}{29.3}$$

$$= 5.54560$$

$$\ln \frac{\bar{f}_1}{x_1} = \ln K_H = \ln f_1 \gamma_1$$

where f_1 is at a solution pressure equal to the vapour pressure of methane and γ_1 is the limiting activity coefficient

$$P = 2.321 \quad {}^{2}/_{0} = 5.119$$

$$\gamma_1 = 0.167$$

$$\ln \frac{\bar{f}_1}{x_1} = \ln (2.321 \times 5.119 \times 0.167)$$

$$= 2.88303$$

$$\frac{\bar{G}_1}{RT} = -5.33 \times (\pi \rho_2 c/6 \, k T \sigma_{12}^{\,3})$$

$$\frac{\epsilon}{k} = 4 \left(\frac{\epsilon_1}{k} \, \frac{\epsilon_2}{k}\right)^{1/2} \sigma_{12}^{\,6}$$

as $\bar{\sigma}_{12} = \sigma_{12}$

Therefore,

$$\frac{\bar{G}_1}{RT} = - \frac{5.33 \times \quad \times 0.025445 \times 6.023 \times 10^{23} \times 4 \times 133.24 \times (3.611 \times 10^{-8})^3}{6 \times 122.66}$$

$$= - 8.75016$$

LITERATURE CITED

1. Bloomer, O. T., and Parent, J. D.,
Chem. Eng. Progr. Symposium Ser., No. 6, 49, 11 (1953).

2. Brown, G. M.,
Ind. Eng. Chem., 51, 472 (1959).

3. Chao, K. C., and Seader, J. D.,
A. I. Ch. E. J., 7, 598 (1961).

4. Cheung, H., and Wang, D. I.-J.,
Ind. Eng. Chem. Fundamentals, 3, 335 (1964).

5. Chang, S.-D.,
M. Sc. Thesis, University of Ottawa, May 1966.

6. Cines, M. R., Roach, J. T., Hogan, R. J., and Roland, C. H.,
Chem. Eng. Progr. Symposium Ser., No. 6, 49, 1 (1953).

7. Davis, J. A., Rodewald, M., and Kurata, F.,
Ind. Eng. Chem., 55, 36 (1963).

8. Deshpande, A. K., and Lu, B. C.-Y.,
J. Chromatog., 12, 539 (1963).

9. Din, F.,
"Thermodynamic Functions of Gases", Butterworth Publications, Vol. 2, p. 181 and Vol. 3, p. 47.

10. Dodge, B. F., and Dunbar, A.,
J. Amer. Chem. Soc., 49, 591 (1927).

11. Eley, D. D.,
Trans. Faraday Soc., 35, 1421 (1939).

12. Fedoritenko, A., and Rubemann, M.,
Tech. Phys. (USSR), 4, 36 (1937).

13. Fowler, R. H., and Guggenheim, E. A.,
"Statistical Thermodynamics", Cambridge 1939, paragraph 823.

14. Hildebrand, J.H., and Scott, R.L.,
"The Solubility of Non-Electrolytes", 3rd Ed., Dover Publications, Chapters VIII and XXIII (1964).

15. Hirschfelder, J.O., Curtiss, C.F., and Bird, R.B.,
"Molecular Theory of Gases and Liquids", John Wiley, New York (1954).

16. Inglis,
Phil. Mag. VI, 11, 640 (1906).

17. Jones, I.W., and Rowlinson, J.R.,
Trans. Faraday Soc., 59, 1702 (1963).

18. Kirkwood, J.G., Lwinson, V.A., and Alder, B.J.,
J. Chem. Phys., 20, 929 (1952).

19. Mathews, and Hurd,
Trans. A.I.Ch.E., 42, 55 (1946).

20. Pierotti, R.A.,
J. Phys. Chem., 67, 1840 (1963).

21. Pitzer, K.S., Lippman, D.Z., Curl, R.F., Huggin, C.M., and Peterson, D.E.,
J. Amer. Chem. Soc., 77, 3433 (1955).

22. Pitzer, K.S., and Curl, R.J. Jr.,
Ind. Eng. Chem., 50, 265 (1958).

23. Prausnitz, J.M.,
A.I.Ch.E.J., 5, 3 (1959).

24. Prausnitz, J.M., and Gunn, R.D.,
A.I.Ch.E.J., 4, 430 (1958).

25. Price, A.R., and Kobayashi, R.,
J. Chem. Engg. Data, 4, 40 (1959).

26. Porter, A.W.,
Trans. Faraday Soc., 16, 336 (1921).

27. Redlich, O., and Kwong, J.N.S.,
Chem. Rev., 44, 233 (1949).

28. Redlich, O., and Dunlop, A. K.,
Chem. Eng. Progr. Symposium Ser., 50, 95 (1963).

29. Redlich, O., Ackerman, F. J., Gunn, R. D., Jacobson, M., and Lau, S.,
Ind. Eng. Chem. Fundamentals, 4, 369 (1965).

30. Redlich, O., Kister, A. T., and Turnquist, C. E.,
Chem. Eng. Progr. Symposium Ser., 48, 49 (1952).

31. Redlich, O.,
Can. J. Chem. Eng., 43, 131 (1965).

32. Reiss, H., Frisch, H. L., and Lebowitz, J. L.,
J. Chem. Phys., 31, 369 (1959).

33. Reiss, H., Frisch, H. L., Helfand, E., and Lebowitz, J. L.,
J. Chem. Phys., 32, 119 (1960).

34. Sage, B. H., and Lacey, W. N.,
Ind. Eng. Chem., 26, 103 (1934).

35. Sage, B. H., and Lacey, W. N.,
Ind. Eng. Chem., 26, 204 (1934).

36. Scatchard, G.,
Chem. Rev., 44, 7 (1949).

36a. Scatchard, G.,
Chem. Rev., 8, 321 (1931).

37. Sprow, F. B., and Prausnitz, J. M.,
A. I. Ch. E. J., 12, 780 (1966).

38. Smith, J. M., Caswell, B., and Shaw, P. V.,
Ind. Eng. Chem., 56, 41 (1964).

39. Smith, J. M., and Caswell, B.,
Ind. Eng. Chem., 57, 45 (1965).

40. Smith, E. B., and Walkley, J.,
J. Phys. Chem., 66, 597 (1962).

41. Sutaman, L. F., and Brown, G. F.,
Chem. Eng. Progr., 45, 139 (1949).

42. Ulig, H. H.,
J. Phys. Chem., 41, 1215 (1937).

43. Van Ness, H. C.,
"Classical Thermodynamics for Nonelectrolyte Solutions",
Pergamon Press, 1964, p. 122.

44. Wagner, I. F., and Weber, J. H.,
Ind. Eng. Chem., Chem. Eng. Data Ser., 3, 220 (1958).

45. Wohl, K.,
Trans. A. I. Ch. E., 42, 215 (1946).

46. Zudkevitch, D., and Kaufmann, T. G.,
A. I. Ch. E. J., 12, 577 (1966).

47. Minthet, V.,
Nuovo Cimento, 9, Suppl. 1, 356 (1958).